

DIRECT CONVERSION OF METHANE TO AROMATICS:
EXPERIMENTAL STUDIES AND QUANTIFIED DATABASE TO OVERCOME THE
DEACTIVATION CHALLENGE

A Thesis

by

NAGAT ELREFAEI

Submitted to the Graduate and Professional School of
Texas A&M University

in partial fulfillment of the requirements for the degree of
MASTER OF SCIENCE

Chair of Committee, Ahmed Abdala

Co-Chair of Committee, Ma'moun Al-Rawashdeh

Committee Members, Luc Vechot

Sherzod Madrahimov

Head of Department, Patrick Linke

December 2021

Major Subject: Chemical Engineering

Copyright 2021 Nagat Elrefaei

ABSTRACT

The methane to aromatics conversion process is one of the non-oxidative methane conversion routes, which does not require the costly and energy-intensive syngas production that is the intermediate step for any methane conversion process. This process is not commercialized due to many challenges, including thermodynamic limitations leading to the low single-pass methane conversion and high-temperature requirement. Another challenge is the rapid catalyst deactivation, as complete catalyst deactivation occurs with few hours of operations. Efficient and fast regeneration of the catalyst that guarantees a continuous process by restoring the catalytic activity and maintain its stability is required. In this work, unconventional regeneration techniques are applied to achieve efficient regeneration and analyze the effect of different molecules (CO_2 and H_2) on the methane dehydroaromatization reaction performed in a fixed bed reactor.

In addition, a quantified database was created to document the historical experimental work done in this field and create a benchmark, help understand the impact of process variables and correlate them, and identify the gaps in the literature to direct future work in this field.

ACKNOWLEDGEMENTS

I would like to thank my Supervisor, Dr. Ma'moun Al-Rawashdeh, for giving me an opportunity to explore the topic. I am thankful to him for his guidance, support, and understanding throughout my journey. Dr. Al-Rawashdeh's has been nothing but helpful from the first day I started working with him, and he made my master's studies an unforgettable experience, and I am grateful to have had the chance to work with him.

I would like to extend my gratitude to my committee members, Dr. Ahmed Abdala and Dr. Luc Vechot, and Dr. Sherzod Madrahimov, who have actively been supportive during my journey.

I would like to thank Dr. Anchu Ashok, who helped me get familiar with all the equipment in the laboratory and for supporting me throughout my master's studies. Dr. Ashok has been a wonderful friend and mentor, and I would not have been able to present this work without her guidance and patience. I would also like to thank Mr. Marcin Kozusznik for his help in building our setup, along with Dr. Al-Rawashdeh and all other laboratory-related issues.

I would like to thank my friends and colleagues at Texas A&M for a great experience in the university while performing my research.

I would like to thank the Office of Graduate Studies (OGAPS) at Texas A&M for their active support and guidance. I would also like to thank the Office of Graduate Studies at Texas A&M at Qatar, especially Mrs. Hania Ayyash, for her unbelievable support and dedication, and Mrs. Cherine Hamed for all the help and support she provided.

I would like to thank my friends for being patient with me throughout and still being there for me whenever I needed them.

Finally, I would like to thank my mother (Dr. Nayera Ismail), my father (Mohamed Elrefaey), my brothers (Aly and Omar), whom I am dedicating this work to, for being understanding, supportive and patient throughout my journey.

CONTRIBUTORS AND FUNDING SOURCES

Contributors

This work was supervised by a thesis committee consisting of Dr. Ma'moun Al-Rawashdeh (co-chair) and evaluated and supported by Dr. Ahmed Abdala (chair), Dr. Luc Vechot (committee member), and Dr. Sherzod Madrahimov (committee member).

The data retrieved for TGA results was conducted in the Chemistry Instrumentation Laboratory at Texas A&M University at Qatar.

All other work conducted for this thesis was completed by the student independently under the direct supervision of Dr. Ma'moun Al-Rawashdeh.

Funding Sources

This research work was made possible by internal startup funding from Texas A&M University at Qatar, and TotalEnergies scholarship in the field of sustainable natural gas conversion to chemical products.

NOMENCLATURE

ΔH_r°	Standard enthalpy of reaction
GC	Gas Chromatograph
g_{cat}	gram of catalyst
HZSM-5	Zeolite
MDA	Methane Dehydroaromatization
Mo	Molybdenum
mol CH ₄	mole fraction of CH ₄
P	Pressure
SV	Space velocity
T	Temperature
TGA	Thermogravimetric Analysis
TOS	Time On Stream
t_{Regen}	Regeneration time
t_{Rxn}	Reaction time
wt%	weight percentage
X	Conversion
Y	Yield

TABLE OF CONTENTS

	Page
ABSTRACT.....	ii
ACKNOWLEDGEMENTS.....	iii
CONTRIBUTORS AND FUNDING SOURCES	v
NOMENCLATURE	vi
TABLE OF CONTENTS.....	vii
LIST OF FIGURES	ix
LIST OF TABLES	xiii
1. INTRODUCTION	1
2. BACKGROUND INFORMATION ABOUT METHANE DEHYDROAROMATIZATION	3
2.1 Thermodynamic Challenge Limiting the Single-Pass Conversion and Explains the Need for High Operating Temperature	4
2.2 Rapid Deactivation Challenge.....	5
2.3 Types of Catalysts and Preparation Methods Used for MDA Reaction	5
2.4 MDA Reaction Mechanism Over Mo/HZSM-5	7
2.5 Forms of Carbonaceous Deposits During MDA Reaction Over Mo/HZSM-5.....	9
2.6 Types of reactors used to perform MDA reaction.....	10
3. THE DEACTIVATION CHALLENGE.....	12
3.1 Conventional Regeneration Techniques.....	12

3.2	Regeneration Through Changing The Feeding Mode.....	14
3.2.1	Continuous Feeding	15
3.2.2	Periodic Feeding	16
3.2.3	Pulse Feeding.....	17
4.	THESIS OBJECTIVES	18
5.	QUANTIFIED DATABASE OF MDA BASED ON LITERATURE STUDIES.....	21
5.1	Methodology of Creating The Quantified Database	21
5.2	Quantified Database Sections and Terminology	22
5.3	Quantified Database Results and Discussion	27
6.	EXPERIMENTAL STUDIES	46
6.1	Experimental Setup	47
6.2	Experimental Procedure	51
6.3	List of Performed Experimental Studies	55
6.3.1	Study 1: Validation – Replicating a Study in Literature.....	56
6.3.2	Study 2: Reproducibility	57
6.3.3	Study 3: Pre-treatment Conditions.....	58
6.3.4	Study 4: Varying Operating Conditions	59
6.3.5	Study 5: Periodic Switch Feeding.....	65
6.3.6	Study 6: Pulse Feeding with H ₂ and CO ₂	76
7.	CONCLUSION AND FUTURE RECOMMENDATIONS	81
8.	REFERENCES	83

LIST OF FIGURES

	Page
Figure 1: Methane conversion routes (Adapted from Ravi et al., 2017)	2
Figure 2: Equilibrium thermodynamics of direct conversion of CH ₄ under nonoxidative (Adapted from Karakaya & Kee, 2016).....	5
Figure 3: Schematic showing the mechanisms of MDA over Mo/HZSM-5 (Adapted from Jeong et al., 2020)	9
Figure 4: Carbonaceous deposits during MDA over Mo/HZSM-5 (Adapted from Zhang, 2019)10	
Figure 5: Circulating fluidized bed reactor (Adapted from Xu et al., 2016)	11
Figure 6: Scheme of the membrane reactor for MDA (Adapted from Xue et al., 2016).....	11
Figure 7: Methane conversion, flow conditions, and temperature for typical regeneration techniques	14
Figure 8: Continuous feeding illustration of the conversion, feed conditions, and temperature ..	15
Figure 9: Periodic feeding illustration of the conversion, feed conditions, and temperature	16
Figure 10: Pulse feeding illustration of the conversion, feed conditions, and temperature	17
Figure 11: Thesis structure.....	18
Figure 12: Example of the database sections	23
Figure 13: Quantified database terminology.....	25
Figure 14: Calculating the D-Slope factor	26
Figure 15: Effect of Mo content on methane conversion, benzene yield, and the D-Slope	29
Figure 16: Effect of Si/Al ratio on methane conversion, benzene yield, and the D-Slope	30

Figure 17: Effect of reaction temperature on methane conversion, benzene yield, and the D-Slope	36
Figure 18: Effect of space velocity on methane conversion, benzene yield, and the D-Slope.....	40
Figure 19: The effect of the change in methane conversion on the benzene yield at pseudo-steady-state	43
Figure 20: Global YC ₆ illustration.....	44
Figure 21: The effect of varying YC ₆ on Global YC ₆	45
Figure 22: YaraCat testing setup.....	47
Figure 23: Mass flow controllers and pressure indicators	48
Figure 24: Temperature controller	48
Figure 25: Safety alarm system.....	49
Figure 26: Gas Chromatograph (Adapted from <i>Nexis GC-2030: SHIMADZU (Shimadzu Corporation)</i> , n.d.).....	50
Figure 27: Circular die used to create a pellet	52
Figure 28: Palletizing machine	52
Figure 29: Mortar and pestle.....	52
Figure 30: Sieves of sizes 300 and 425 μ m	52
Figure 31: Loaded reactor inserted into the furnace	53
Figure 32: (a) CH ₄ conversion (b) and C ₆ yield of this work compared to literature	56
Figure 33: (a) CH ₄ conversion (b) and C ₆ yield of reproducibility studies	57
Figure 34: (a) CH ₄ conversion (b) and C ₆ yield for different pre-treatment conditions	59
Figure 35: (a) CH ₄ conversion (b) and C ₆ yield for different space velocities	60

Figure 36: (a) CH ₄ conversion (b) and C ₆ yield for different reaction temperatures.....	61
Figure 37: TGA Analysis of spent 6wt% Mo/HZSM-5.....	62
Figure 38: (a) CH ₄ conversion (b) and C ₆ yield for reference experiment with continuous CH ₄ feed	66
Figure 39: (a) CH ₄ conversion (b) and C ₆ yield for Reference experiment and 45-45 (min) CH ₄ -H ₂ periodic switch.....	67
Figure 40: (a) CH ₄ conversion (b) and C ₆ yield for Reference experiment and 45-45 and 45-15 (min) CH ₄ -H ₂ periodic switch.....	68
Figure 41: Illustration of the different sampling time (ST1 and ST2) during periodic switch.....	69
Figure 42: (a) CH ₄ conversion (b) and C ₆ yield for different sampling times.....	70
Figure 43: (a) CH ₄ conversion (b) and C ₆ yield for Reference experiment and 45-45 and 15-5 (min) CH ₄ -H ₂ periodic switch.....	71
Figure 44: (a) CH ₄ conversion (b) and C ₆ yield for Reference experiment and 15-1, 15-2.5, 15-5, 15-10 (min) CH ₄ -H ₂ periodic switch.....	71
Figure 45: (a) CH ₄ conversion (b) and C ₆ yield for Reference experiment and 45-45 (min) CH ₄ - CO ₂ periodic switch.....	73
Figure 46: (a) CH ₄ conversion (b) and C ₆ yield for Reference experiment and 45-45, 15-45, and 15-5 (min) CH ₄ -CO ₂ periodic switch.....	74
Figure 47: (a) CH ₄ conversion (b) and C ₆ yield for Reference experiment and 45-45 (min) CH ₄ - H ₂ + CO ₂ periodic switch.....	75
Figure 48: (a) CH ₄ conversion (b) and C ₆ yield for Reference experiment and H ₂ pulsing with 0.3, 1.5, and 3.5 min frequencies.....	77

Figure 49: (a) CH₄ conversion (b) and C₆ yield for Reference experiment and 15-1 (min) CH₄-H₂ periodic switch and H₂ pulsing with frequency of 3.5 min..... 78

Figure 50: (a) CH₄ conversion (b) and C₆ yield for Reference experiment and CO₂ pulsing with 0.25, 2, 3.5, 5, and 10 mins frequencies..... 79

LIST OF TABLES

	Page
Table 1: Comparison of zeolite supports for Mo-based MDA catalysts (Adapted from Ma et al., 2013)	6
Table 2: Definition of database terminology shown in Figure 13	24
Table 3: List of filters applied to the database for each variable	42
Table 4: Experimental studies performed in this work.....	55
Table 5: Reaction conditions for study no. 1	56
Table 6: Reaction conditions for study no. 2	57
Table 7: Summary of TGA results for study no. 4	63

1. INTRODUCTION

Methane forms 95% of natural gas, which is the most abundant source of fossil fuel distributed around the world (Kosinov & Hensen, 2020). Methane is also an extremely important feedstock for production of value-added chemicals. While it is currently the cleanest hydrocarbon fuel, the processes through which it is being utilized emits many gases that significantly impact the environment. Therefore, it is essential to explore the utilization of methane through more sustainable routes.

Figure 1 presents the different routes that methane can be utilized to make platform chemicals, which include indirect routes (syngas-based) and direct routes (Ravi, Ranocchiari, & van Bokhoven, 2017). The only commercialized methane utilization processes are indirect ones using syngas production. Most of these processes start with one of the reforming reactions, which produce 9-14 kg CO₂/ kg H₂ based on the reaction stoichiometry (Dagle et al., 2017). The syngas production step is thermodynamically favored; however, it requires large capital costs as a result of technical complexity (Taifan & Baltrusaitis, 2016). Moreover, it requires high temperature and high pressure, which as a result, emits a significant amount of CO₂ (L. Sun, Wang, Guan, & Li, 2019). Recently, significant efforts have been made towards the commercialization of direct conversion of methane processes, to simplify the process and reduce its CO₂ emissions.

The direct conversion processes, the non-oxidative route does not require oxygen to form the final products, reducing the total CO₂ emissions and eliminating the possibility of its formation through reaction stoichiometry.

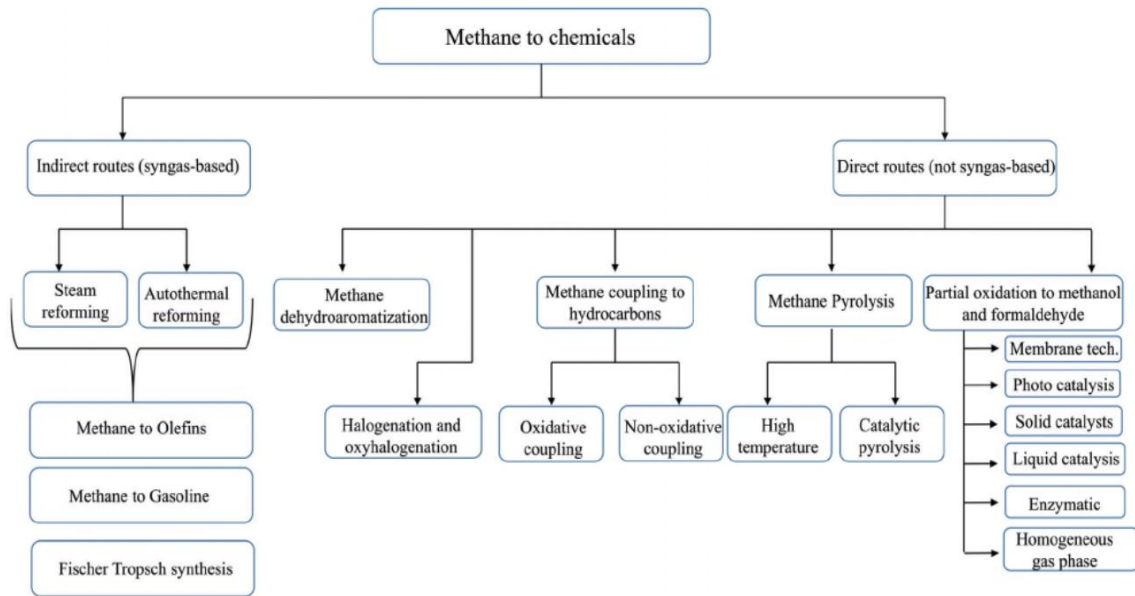
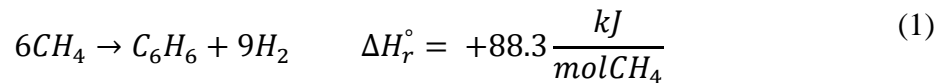


Figure 1: Methane conversion routes (Adapted from Ravi et al., 2017)

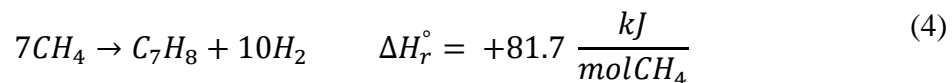
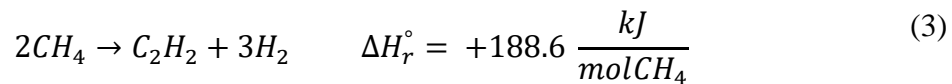
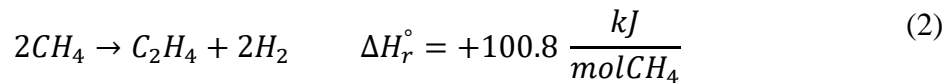
One of the direct conversion processes is the conversion of methane to aromatics, also known as the methane dehydroaromatization (MDA) process. This process produces mainly benzene and other aromatics such as toluene, xylene, and naphthalene in smaller amounts. Although benzene is very crucial for the production of polystyrene and other goods, currently, benzene, toluene, and xylene (BTX) are being produced as by-products through the catalytic steam reforming of naphtha. This process is being challenged with the rise of shale gas, leading to building large-scale ethane crackers that do not produce aromatics; therefore, it is essential to start exploring other resources for aromatics production (Vollmer, Yarulina, Kapteijn, & Gascon, 2019).

2. BACKGROUND INFORMATION ABOUT METHANE DEHYDROAROMATIZATION

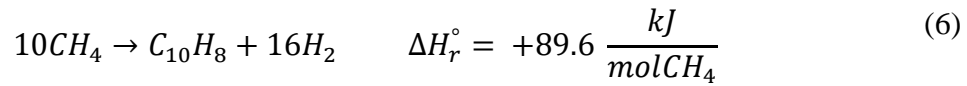
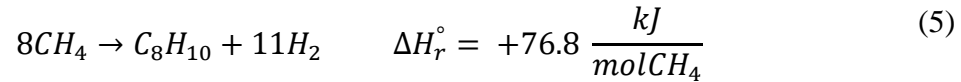
This section is a literature review of the chemistry behind the methane dehydroaromatization (MDA) reaction, the typical process conditions, and the challenges hindering the process from commercialization. Methane dehydroaromatization reaction is one of the non-oxidative direct routes to convert methane to value-added chemicals. The main reaction in this process is as follows:¹



The reaction takes place at higher temperatures (>500°C) and atmospheric pressure, during which the C-H bond in the methane molecule breaks and aromatic products and hydrogen form. Other reactions may also take place during the MDA process forming other aromatics products such as toluene, xylene, and naphthalene, as well as ethylene and acetylene as intermediate products (Vollmer, Yarulina, Kapteijn, & Gascon, 2019).



¹ All the values for heat of reaction were obtained from Aspen plus using RStoic reactor.



The processes mentioned above produce desired products; however, they also produce carbon which is considered, in this case, as an undesired product because it blocks the catalysts and makes them inactive.



2.1 Thermodynamic Challenge Limiting the Single-Pass Conversion and Explains the Need for High Operating Temperature

The above thermodynamic analysis shows that the low equilibrium conversion thermodynamically limits the process even at very high reaction temperatures. For example, at a reaction temperature of 700°C and atmospheric pressure, the maximum methane conversion to benzene and hydrogen is ~ 11.8%. This low conversion requires separation units and large recycle streams, which could make the process uneconomical.

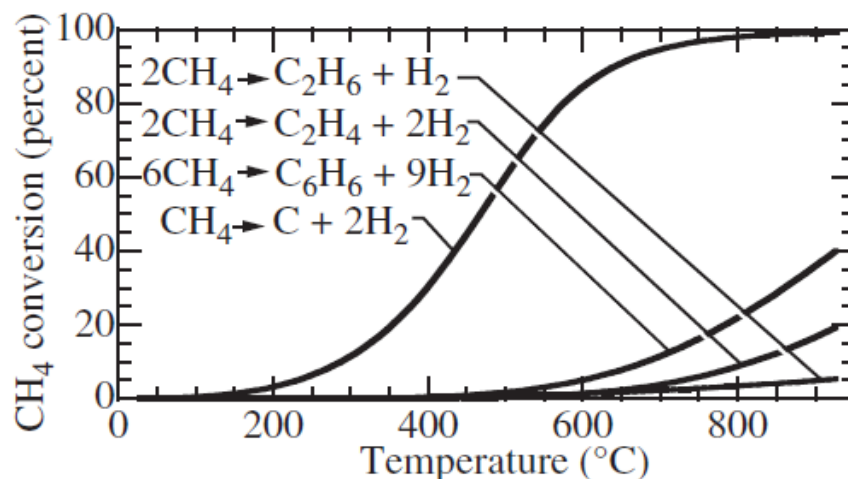


Figure 2: Equilibrium thermodynamics of direct conversion of CH₄ under nonoxidative (Adapted from Karakaya & Kee, 2016)

2.2 Rapid Deactivation Challenge

At the given operating conditions, coke formation is more thermodynamically favorable than benzene and other aromatics products, as demonstrated in **Figure 2** (Karakaya & Kee, 2016). Coke formation is also an extremely fast reaction causing a complete catalyst deactivation within hours of reaction time. This stops the main reaction because the coke covers the active sites or accumulating inside the catalyst pores preventing methane from accessing those active sites. However, before discussing types of carbonaceous depositions, it is crucial first to discuss the catalysts used for this process.

2.3 Catalysts and Preparation Methods Used for MDA Reaction

Over the years, many catalysts have been tested for the MDA reaction, and so far, Mo-based zeolites catalysts have been the most studied catalysts while also resulting in the best

performance. Zeolites are solid, super-acidic, microporous catalysts with well-defined structures (Schwach, Pan, & Bao, 2017). A zeolite framework generally consists of silicon, aluminum, oxygen, and cations or water in its pores (Majhi & Mohanty, 2013). Zeolites are also very unique as their pore size is close to the size of benzene molecules (Yide Xu & Lin, 1999).

The following **Table 1** compares the performance of different zeolites for MDA reaction (Ma, Guo, Zhao, & Scott, 2013). Although HZSM-5 is not the best zeolite for MDA reaction, it is the most widely studied. Some studies attempted to improve the catalytic performance by adding other metals to Mo/HZSM-5 zeolite, such as; Co, Ni (Sridhar et al., 2020), Ce, Mn (Fila, Bernauer, Bernauer, & Sobalik, 2015), Fe (Yuebing Xu, Wang, Suzuki, & Zhang, 2012), Cr, W, Ru, Pd, Zn (Aboul-Gheit & Awadallah, 2009), and Cu (Qi & Yang, 2004).

Table 1: Comparison of zeolite supports for Mo-based MDA catalysts (Adapted from Ma et al., 2013)

Zeolites	Pore size (Å)	MR	Reaction conditions		CH ₄ conversion (%)	Selectivity (%)			Reference
			temperature (°C)	flow (mL.g _{cat} ⁻¹ .h ⁻¹)		C ₆ H ₆	C ₁₀ H ₈	coke	
HZSM-5	5.4×5.6, 5.1×5.5	10	700	1500	10.0	58.2	18.2	16.5	[33]
				1600	5.9	91.3 ^a	–	–	[10]
HZSM-8	5+	10		1600	8.0	90.1 ^a	–	–	[10]
HZSM-11	5.1×5.5	10		1600	4.1	86.7 ^a	–	–	[10]
HMCM-22	4.0×5.5, 4.1×5.1, 7.1×7.1	10, 12		1500	9.9	72.8	5.9	13.0	[33, [34]
HMCM-41	4.0			1600	0.9	80.1b ^b	0	–	[10]
HMCM-36				1500	11.5	47.4	0.31	28.5	[49]
HMCM-49	4.0×5.9, 4.0×5.4	10		1500	13.0	76.9	5	3.54	[43]
NU-87	4.8×5.7	10, 12		1500	11.0	22.9	10.9	62.7	[50]
HZRP-1	5.0×5.3, 5.0×5.4	10		1500	9.7	48.6	27.0	13.9	[55] [56]
ITQ-2		6, 10		1500	7.1	70	20	10	[52]
ITQ-13	4.0×4.9, 4.8×5.7, 4.7×5.1	9, 10, 10		1500	2.0	72 ^b	12	–	[53]
HMCM-56				1320	6.5	52	–	30	[54]
IM-5	5.5×5.6, 5.3×5.4, 5.3×5.9, 4.8×5.4, 5.1×5.3	10		1500	11.5	39.3	14.6	5.2	[57]
TNU-9	5.2×6.0, 5.1×5.5, 5.4×5.5, 7.2×7.2	10, 12		1500	11.3	81.2 ^b	16.6	–	[58]

Metals are usually added to the zeolite base through impregnation, also known as incipient wetness impregnation (IWI); however, some other preparation methods are also reported. For example, Aboul-Gheit & Awadallah (2009) prepared W+Mo/HZSM-5 and Cr+Mo/HZSM-5 catalysts using mechanical mixing. Another example is Yuebing Xu et al. (2020), who used the ion exchange method to add Ni to HZSM-5 zeolite. Finally, Julian et al. (2020) used the supercritical solvothermal synthesis method to prepare Mo/HZSM-5 catalyst.

2.4 MDA Reaction Mechanism Over Mo/HZSM-5

This work will focus on MDA reaction over Mo/HZSM-5 catalyst. Once Mo is added into the zeolite, it is assumed to exist in several oxide forms on the surface of the catalyst and inside the catalyst pore. The nature of the metal (Mo) precursor determines the number of active sites available in the catalyst. Many factors determine the nature of the precursor, such as the zeolite Si/Al ratio, the preparation method, and the Mo loading wt%. The most common form of Mo-oxo is believed to be MoO₃; however, it is suggested that after MoO₃ diffuses into the zeolite pore, it takes one of the two forms MoO₂²⁺ monomer or Mo₂O₅²⁺ (dimer) (Kosinov & Hensen, 2020). Some consider Mo monomers the preferred form of Mo-oxide as they link with the zeolite wall on two Brønsted acid sites rather than one, in the case of Mo dimers. This allows the Mo atom to have a stronger bond with the zeolite and reduces its likelihood of sintering (Tessonnier, Louis, Rigolet, Ledoux, & Pham-Huu, 2008).

MDA reaction over Mo/HZSM-5 goes through three main stages; induction, pseudo/ quasi-steady-state, deactivation (Kosinov & Hensen, 2020). The induction period is the stage during which methane reacts with Mo oxide forming the active metal site Mo₂C, and it lasts about 30

mins or more. It is assumed that all Mo oxide converts to Mo carbide by the end of the induction period. CO, CO₂, and H₂, along with unconverted CH₄, are the gas products in this stage.

The second stage is the pseudo-steady-state which is assumed to be a very short period during which the MDA reaction starts, and aromatics production begins.

The third and last stage is the reaction/ deactivation stage associated with the start of coke formation taking place simultaneously with the MDA reaction causing CH₄ conversion to decrease rapidly until eventually the catalyst completely deactivates and methane conversion can no longer take place. This period is assumed to last a few hours, depending on the type of catalyst, reaction conditions, and feed compositions.

The generally acceptable reaction mechanism of MDA over Mo/HZSM-5 is called the bifunctional mechanism, which assumes that the catalyst has a bifunctional nature. **Figure 3** demonstrates the reaction steps taking place in this mechanism (Jeong, Hwang, Kim, Hong, & Park, 2020). The first function is activating the C-H bond in the methane molecule, which is performed by the active metal site (Mo₂C) resulting in intermediate C₂ molecules, for example, ethane and ethylene. The second function is the formation of aromatic compounds over the Brønsted acid sites of the zeolite (Vollmer et al., 2019).

The second mechanism, hydrocarbon pool, is mostly assumed for the methanol to olefins process, generally considering that methane is activated on the metal site, similarly to the bifunctional mechanism. Then, the unreacted methane and intermediate C₂ molecules convert into radical species, which then enter the zeolite pore and contribute to the formation of polyaromatics inside the pores. This can cause a build-up of the hydrocarbon pool inside the pore until the pool

is appropriately developed to produce benzene (Uslamin, Saito, Sekine, Hensen, & Kosinov, 2020).

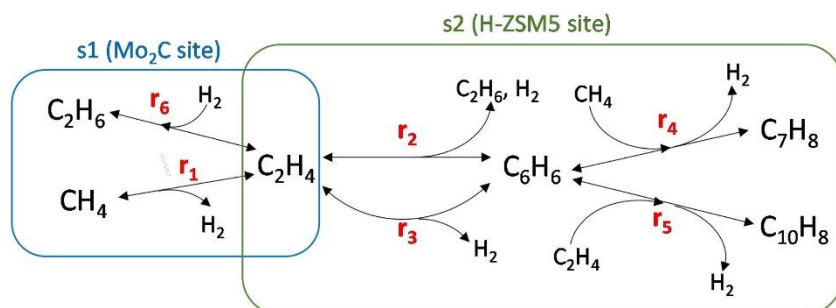


Figure 3: Schematic showing the mechanisms of MDA over Mo/HZSM-5

(Adapted from Jeong et al., 2020)

2.5 Forms of Carbonaceous Deposits During MDA Reaction Over Mo/HZSM-5

Carbonaceous deposits forming during MDA reaction over Mo/HZSM-5 catalyst can be classified into three different forms and locations, presented in the schematic in **Figure 4** (Zhang, 2019). The first is the carbide type which forms when methane converts the Mo oxide to Mo carbide during the induction period. The second type is the hard coke located inside the catalyst pore, on either the acid or metal sites. This type is harder to remove, according to a recent study done by Han et al. (2019). The third and final type is the soft coke forms on the catalyst's external surface (Zinfer R. Ismagilov, Matus, & Tsikoza, 2008).

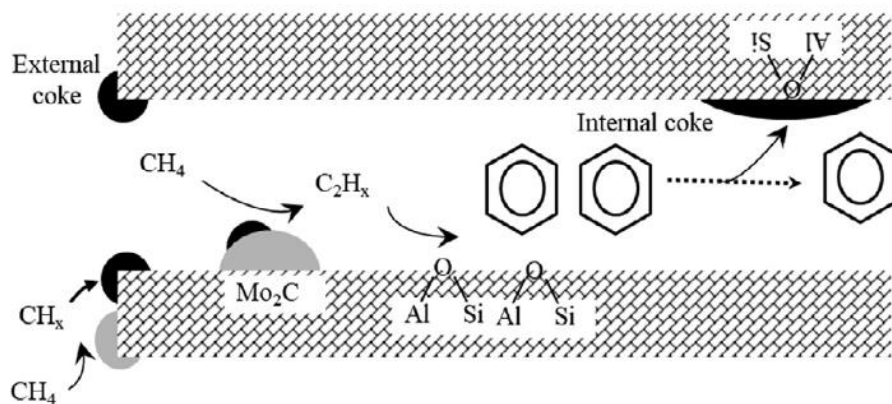


Figure 4: Carbonaceous deposits during MDA over Mo/HZSM-5 (Adapted from Zhang, 2019)

2.6 Types of reactors used to perform MDA reaction

The MDA reaction can be carried out in different reactor designs, and each has its advantages and drawbacks.

Fixed bed reactors

Most reported MDA work uses fixed bed reactor mainly because this technology is still at the laboratory stage. Nonetheless, reactions in fixed bed reactors face many challenges when scaled to an industrial scale as they are limited by the maximum single-pass equilibrium conversion allowed by thermodynamics. In addition, the fact that once the bed is deactivated, an offline regeneration is required. Therefore, multiple parallel reactors are needed to maintain continuous operation. Thus, researchers started to test MDA chemistry in other reactor designs.

Fluidized bed reactors

The fluidized bed reactor design holds a major advantage over the fixed bed reactor as it allows continuous and efficient regeneration of the catalyst and permitting a continuous operation. Yuebing Xu et al. (2016) developed a circulating fluidized bed reactor (CFBR) with two beds to separately perform reaction and regeneration. In this study, the system was continuously tested for four days; however, the results were not much different from the performance achieved in a conventional fixed bed reactor. This was attributed to the much higher space velocity used in CFBRs than the fixed bed reactor, causing a much faster deactivation.

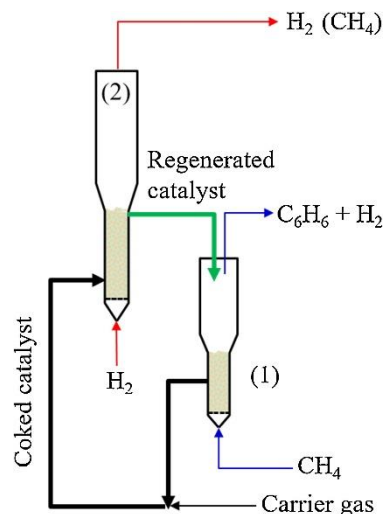


Figure 5: Circulating fluidized bed reactor (Adapted from Xu et al., 2016)

Membrane reactors

Another proposed type of reactor is the membrane reactor that can overcome the low single-pass conversion challenge by selectively removing the hydrogen to shift the equilibrium in the forward direction. Xue et al. (2016) developed a membrane reactor using 6 wt% Mo/HZSM-5 to coat the outside of a fiber membrane, which removed 40-60% of H₂ produced by introducing CO₂. However, this increased the coke formation by 10% compared to fixed bed reactors.

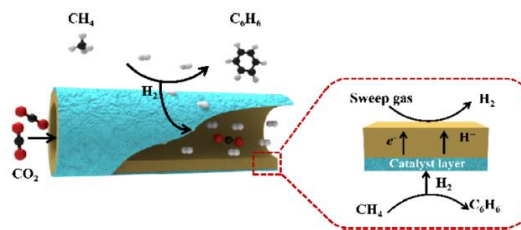


Figure 6: Scheme of the membrane reactor for MDA (Adapted from Xue et al., 2016)

Other reactor design

Other reactor types were applied, such as plasma reactors, triple-bed CFBR, and two-zone fluidized bed reactors. However, this work will solely focus on fixed bed reactor applications.

3. OVERCOMING THE DEACTIVATION CHALLENGE

As discussed in the previous section, catalytic deactivation is a major challenge associated with the MDA process. The main effect of deactivation on the catalytic performance can be seen from the decrease in methane conversion and the decrease in the product yield.

3.1 Conventional Regeneration Techniques

One way to overcome the deactivation challenge is to regenerate the catalyst once it deactivates completely in a separate subsequent step, as shown in **Figure 7**. Two types of regeneration molecules can be used to carry reductive regeneration and oxidative regeneration. Reductive regeneration is based on feeding a reducing molecule H_2 to react with coke and remove it, producing methane according to Eq. (8) (C. Sun et al., 2015).



Regenerating with H_2 is effective in maintaining a somewhat stable performance for up to tens of hours. For example, the work of Sridhar et al. (2020) demonstrated a stable performance for 27h.

Oxidative regeneration is based on feeding an oxidative molecule, which can be pure O₂, CO, or CO₂. The oxidizing molecule aims to burn coke. If O₂ is used, it is believed that the mechanism can be expressed by Eq. (9) and (10) (Han et al., 2019).



CO₂ can, in principle, be used as a regeneration molecule. According to Eq. (11) (Liu, Kooli, & Borgna, 2019).



CO can also be used as regenerating molecules. When CO comes in contact with Mo sites, it can dissociate into C, forming an intermediate CH_x, while the O molecule can react with the formed coke to produce CO or CO₂, which helps suppress the coke formation (Yide Xu, Bao, & Lin, 2003).

(Han et al., 2019) carried a detailed study on the optimum conditions for each regeneration type and found that for a reaction temperature of 700°C, regenerating under reducing conditions (H₂ flow) requires increasing the temperature to 800°C to achieve the most activity recovery. However, even at such high a temperature, there is a clear decrease in the reactivity and stability due to metal sintering as well as hard coke accumulation which is enhanced by the high temperature. In the same study, the conditions for oxidative regeneration using O₂ were tested. The optimal temperature for regeneration was at 450°C, which is much lower than the reaction temperature. When performing oxidative regeneration at the reaction temperature or higher, there is a clear decrease in the methane conversion and benzene yield after every regeneration cycle. This is believed to be the result of metal sintering and the severe irreversible deactivation of acid

sites which was evident by increasing selectivity toward ethylene. Ethylene is the intermediate product, which indicates that after its formation, the number of available acid sites that could convert it into aromatics decreased. **Figure 7** shows a schematic example of how deactivation and regeneration occur if each step was carried out separately. During regeneration, flow rate and feed composition can be adjusted as needed.

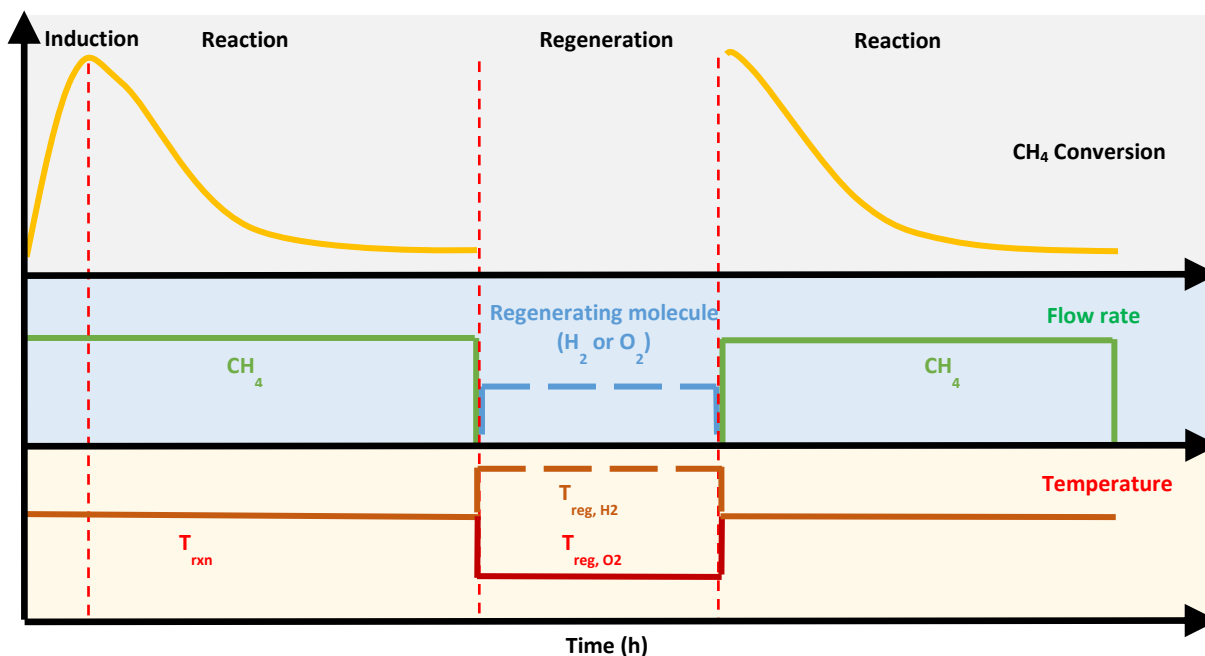


Figure 7: Methane conversion, flow conditions, and temperature for typical regeneration techniques

3.2 Regeneration Through Changing The Feeding Mode

Other regeneration approaches are proposed in the literature to maximize the production rate and avoid demanding temperature switches between reaction and regeneration cycles. This could be achieved by co-feeding other molecules to carry out regeneration much earlier in the reaction

cycle and minimizing the coke formation. This can be done in different three different feeding modes, as stated below.

3.2.1 Continuous Feeding

The first feeding mode is continuous feeding, which means that we continuously feed another molecule alongside methane throughout the reaction time. The advantage of this method is it can continuously react with the catalyst and remove the coke as it is being formed, preventing its accumulation. It can also help decrease the deactivation rate. **Figure 8** shows the theoretical conversion curve when introducing other molecules while maintaining the reaction temperature.

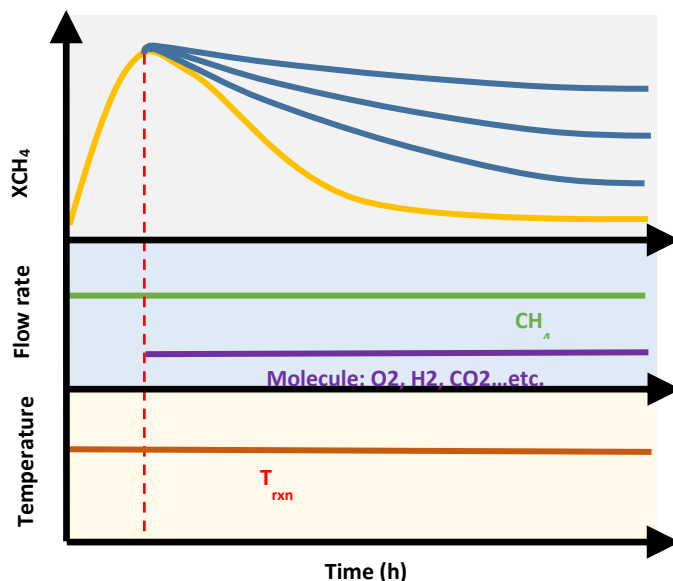


Figure 8: Continuous feeding illustration of the conversion, feed conditions, and temperature

Many molecules have been continuously fed with methane during the MDA reaction. One of which is continuously feeding O_2 in very small quantities not exceeding 2% of the feed gas (Li et

al., 2003). (Chen et al., 2020) introduced CO with 2-10% of the feed gas. Other studies introduced CO₂, H₂, C₂H₄, C₂H₆, H₂O, and CH₃OH.

3.2.2 Periodic Feeding

The second mode is periodic feeding in which the feed is switched between methane and the regenerating molecule within minutes. Similar to continuous feeding, this aims to remove the coke before it accumulates and decrease the conversion dramatically and before the irreversible coke starts forming. **Figure 9** illustrates the periodic feeding process, allowing switching between the two feed gases while maintaining the same temperature.

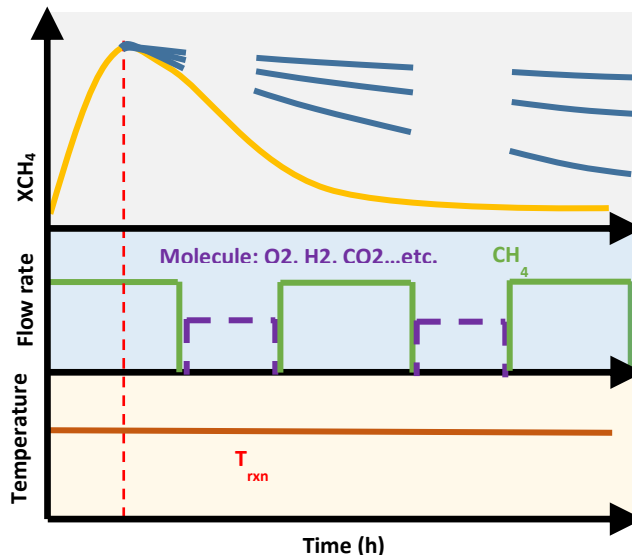


Figure 9: Periodic feeding illustration of the conversion, feed conditions, and temperature

CH₄-H₂ periodic switch is the most studied in periodic feeding gas as, it proved its ability to achieve stable performance and efficient regeneration in many studies (Honda, Yoshida, & Zhang, 2003), (Yuebing Xu et al., 2012), (Yuebing Xu, Lu, Wang, Suzuki, & Zhang, 2011), (C. Sun et

al., 2015). Other studies explored the effect of periodically feeding O₂ with a periodic switch frequency of CH₄-O₂ (90-30) mins (Portilla, Llopis, & Martínez, 2015), which showed promising results maintaining a stable performance for 18h. However, there was a need to lower the temperature from 700°C to 540°C during the regeneration period.

3.2.3 Pulse Feeding

The third and last mode is pulse feeding which is very similar to periodic feeding; however, in pulse feeding, the pulsing of the second molecule is more frequent, and the methane feed is continuous. As illustrated in **Figure 10**, the temperature and the methane flow rate are maintained constant while the regeneration gas is pulsed every few minutes. Pulse feeding was applied for the MDA reaction using O₂, and it showed a decrease in the deactivation rate. This helped extend the reaction time from 8h (no regeneration gas) to 16h (Kosinov, Coumans, Uslamin, Kapteijn, & Hensen, 2016).

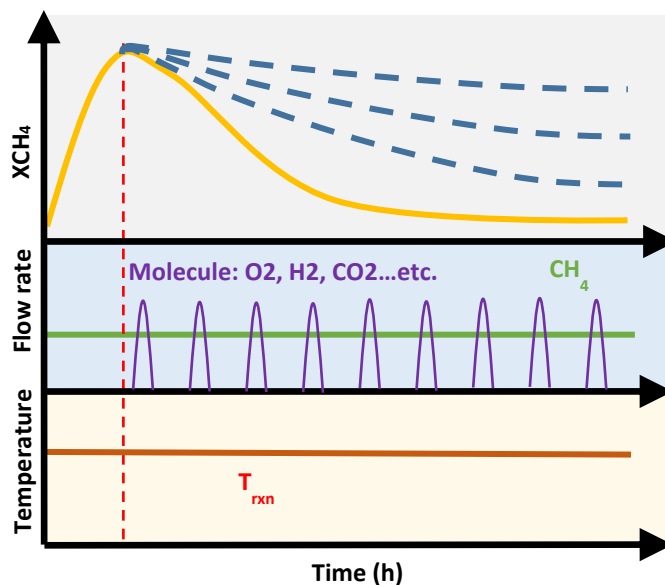


Figure 10: Pulse feeding illustration of the conversion, feed conditions, and temperature

4. THESIS OBJECTIVES

In this work, periodic and pulse feeding of CO_2 and H_2 will be explored as unconventional regeneration techniques towards achieving an efficient regeneration and a continuous process for the methane dehydroaromatization reaction, addressing the challenge of deactivation. To achieve that, literature data were quantified and analyzed, and the gaps were identified in order to guide the experimental work.

This thesis will have two main routes, as shown in **Figure 11**. The first is a quantified database that analyzes the historical literature work in this field. The second is the experimental route carried out in a fixed bed quartz reactor in the Catalytic Reactor Laboratory. The objectives of each route are provided below. Afterward, the methodology used in both routes will be explained followed by the results and conclusions.

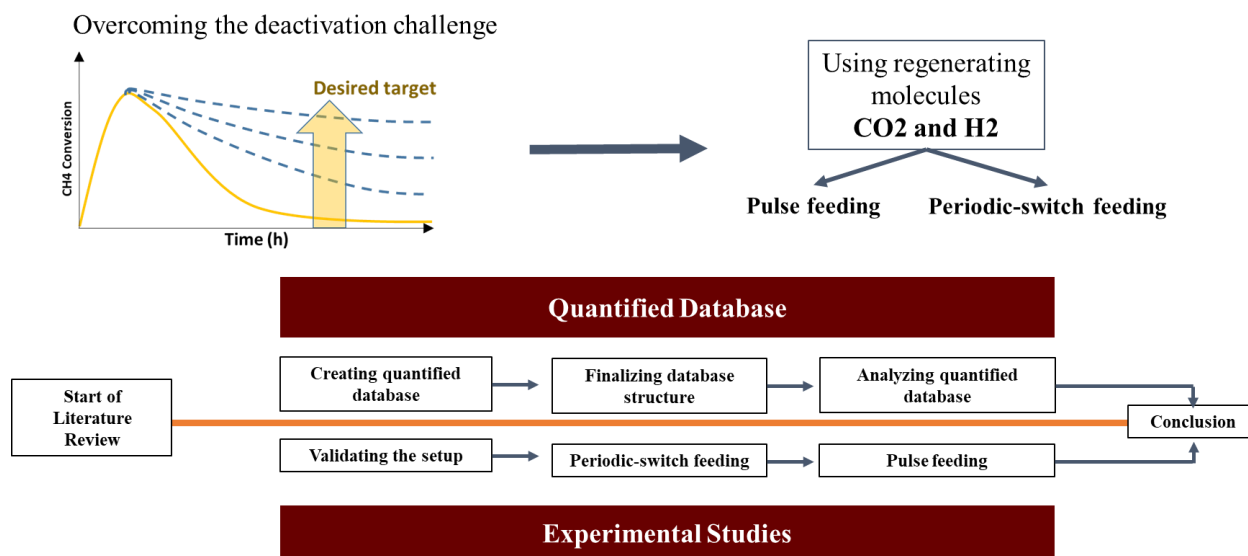


Figure 11: Thesis structure

Quantified database route:

An intensive literature review was performed as part of this work to understand the MDA process and its challenges. Initially, a qualitative database was created and analyzed to direct the research focus and identify the gaps in the literature. A significant number of studies were found in the literature but with isolated results with no clear and definite conclusions. Therefore, this thesis's first aim was to establish a quantified database to analyze the reported work better and create a benchmark for future research direction.

The motivation behind creating a quantified database for the MDA reaction

- This topic is of high importance with numerous articles already published
- Establishing correlations through experimental studies is time-consuming due to the nature of the reactions involving rapid deactivations and long-term stability issues
- Establish a distinct benchmark for future studies
- Identify the parameters or combination of parameters having the strongest impact on the MDA reaction
- Discover potential areas of research by identifying the missing information
- Motivating researchers from data science to explore this reaction application and show what can be achieved using these new methods

Experimental studies route:

The experimental plan for this work is divided into multiple sections. The first section includes the validation experiments performed to validate the operability of the setup by replicating published work and validate the results. The second and third sections include the

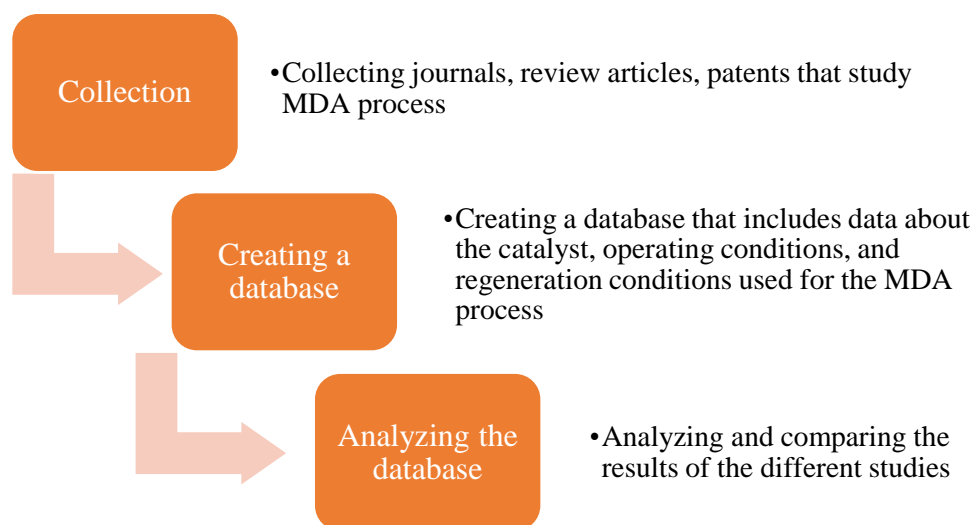
periodic switch and pulse feeding experiments with the aim to maintain a stable and relatively high performance during the first reaction cycle and maximize the recovery of the activity after the regeneration cycle.

Two molecules were selected for these studies. The first being H_2 , which will perform the function of reductive regeneration. H_2 was selected as it is a by-product of many reforming processes, and it has proven its efficiency when being introduced for a long time in a separate regeneration step. The second regeneration molecule is CO_2 which is reportedly a good oxidant when continuously fed to the MDA reaction in minor amounts.

5. QUANTIFIED DATABASE OF MDA BASED ON LITERATURE STUDIES

5.1 Methodology of Creating the Quantified Database

The creation of the quantified database happened over two stages. First is the creation of a database, which included information about the different studies in a qualitative manner. This process consisted of three main steps as explained below.



- From the collection step about 300 articles, 20 review papers, and 100 patents were found about the direct conversion of methane to aromatics. Following that, it was clear that there are many studies in this field, but at the same time fragmented with some common conclusions. About 100 articles were selected out of which 40 were analyzed as they had similar reported data. The following were observed: Difficulties in comparing the results (no indication of the long-term stability)

- Different studies test different ranges; therefore, the optimum conditions are difficult to identify
- After analyzing the literature data, it was observed that only very few studies report sufficient data
- Performance parameters are calculated differently, which makes direct comparison not straightforward

Based on the above we decided to create a quantified database to help advance this application and overcome the challenges mentioned above.

5.2 Quantified Database Sections and Terminology

The quantified database was divided into sections, each addressing a certain group of variables as shown in **Figure 12**.

Section 1: The catalyst type, metal composition, Si/Al ratio (specific for zeolites), particle size, and preparation method

Section 2: Operating conditions (reaction space velocity, reaction temperature, reaction pressure), feed composition (including any co-fed molecules), periodic switch feeding (composition, switch frequency, regeneration period), pulse feeding (composition and pulse frequency)

Section 3: Regeneration conditions; feed composition, regeneration space velocity, regeneration temperature, regeneration pressure, regeneration period

Section 4: Product analysis (at specific TOS); methane conversion, products yield, products selectivity

Catalyst and metal	Catalyst									
	Metals									
	Catalyst name	metal 1 (Mo)	metal 2 (Ce)	metal 3 (Co)	metal 4 (Mn)	Si/Al	SiO2/Al2O3	Particle size	Preparation method	
	(-)	wt%	wt%	wt%	wt%	(-)	(-)	(μm)	(-)	
	Mo/HZSM5	2	-	-	-	13	26	250-500	IWI	
	Mo/HZSM5	3	-	-	-	13	26	250-500	IWI	

Operating conditions			Inlet compositions					Pulse conditions				Periodic Switch conditions						
GHSV	Temperature	Pressure	CH4	inert (Ar, N2, He)	cont. 1 (O2)	cont. 2 (H2)	cont. 3 (CO2)	Compositions				Compositions						
								O2	CO2	V	freq.	H2	O2	He/Ar	CH4	GHSV	rxn period	regen. period
ml/g/h	$^{\circ}\text{C}$	bar	(-)	(-)	(-)	(-)	(-)	(-)	(-)	ml	min	(-)	(-)	(-)	(-)	ml/g/h	min	min
1800	700	1	0.95	0.05	-	-	-	1	-	2	12	-	-	-	-	-	-	-
1800	700	1	0.95	0.05	-	-	-	1	-	2	3	-	-	-	-	-	-	

pseudo st st										Point 1					
TOS	X CH4	yC6	SC6	SC7	SC8	SC10	SH2	Y Aromatics	S Aromatics	TOS 1	X CH42	Y C6	S C6	Y Aromatics	S Aromatics
min	%	%	%	%	%	%	%	%	%	h	%	%	%	%	%
45	16.5	8	-	-	-	-	-	-	-	1.7	13.5	8	-	-	-
45	17	9	-	-	-	-	-	-	-	3.3	14.5	8.5	-	-	-

Regen conditions							pseudo st st2						pseudo st st3					
Compositions																		
T	P	GHSV	air	H2	inert (N2, He)	Duration	TOS1	XCH424	Y C6	S C6	S C10	Y Aromatics	TOS1	X CH4	Y C6	S C6	S C10	Y Aromatics
$^{\circ}\text{C}$	bar	cm3/g/h	(-)	(-)	(-)	h	h	%	%	%	%	%	h	%	%	%	%	%
765	-	2400	-	1	-	2	200	14	8	60	15	11	280	13	7.5	60	15	10
530	1	-	1	-	-	2	6	12.5	6.5	-	-	-	10	9	5	-	-	-

Figure 12: Example of the database sections

Several terminologies were defined to report comparable results. In addition to that, these terminologies showed how the deactivation happened in each study by defining specific time points and reporting the performance parameters (conversion, yield, selectivity) at these time points, as shown in **Table 2**.

Table 2: Definition of database terminology shown in Figure 13

Terminology	Explanation	How it is defined
<i>TOS</i>	Time on stream	The total time on stream from starting when the catalyst is being exposed to ramping feed gas till the end of the test, including any regeneration activities
<i>SI</i>	The point of pseudo-steady-state at the first reaction cycle	The point in time at which the level of benzene yield (being the most selective product after coke) reaches a peak
<i>D1</i>	The initial deactivation datapoint	Different points in times along the deactivation of the first cycle
<i>D2</i>	The middle deactivation datapoint	
<i>D3</i>	The end deactivation datapoint	The last reported point at the end of the first reaction cycle after deactivation
<i>SM</i>	The point of pseudo-steady-state for an intermediate reaction cycle	The point in time at which the level of benzene yield reaches a maximum in an intermediate reaction cycle
<i>SF</i>	The point of pseudo-steady-state for the last reported reaction cycle	The point in time at which the level of benzene yield reaches a maximum in the last reported reaction cycle

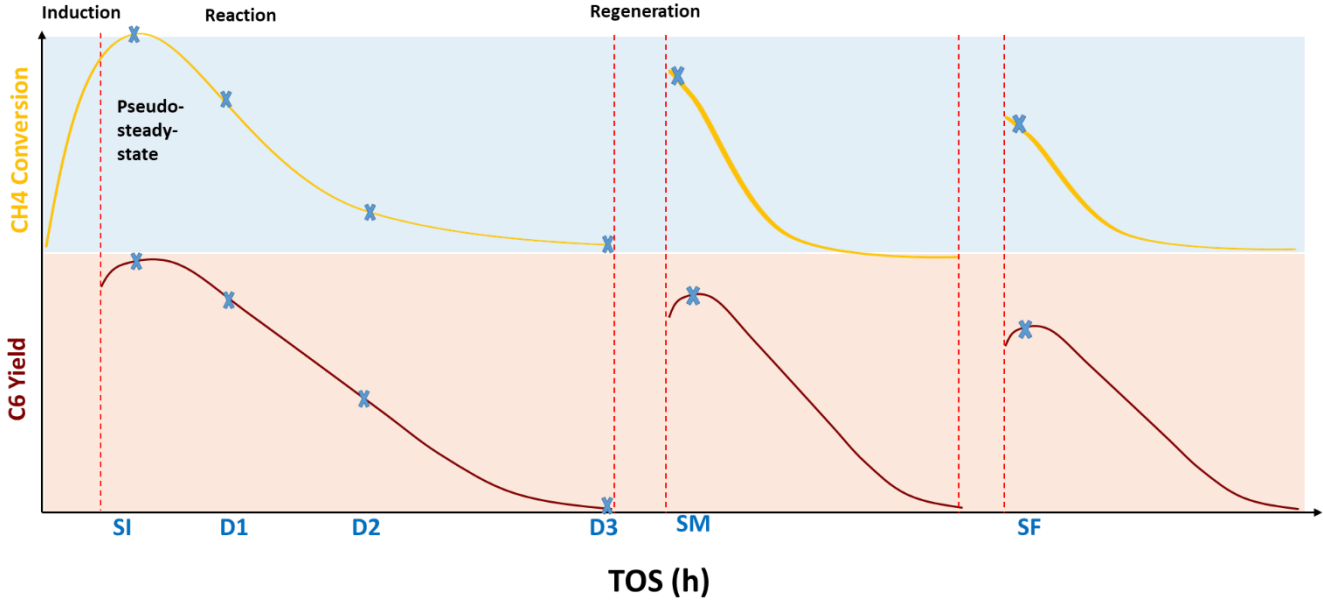


Figure 13: Quantified database terminology

To allow analyzing the database, the definitions of the following parameters were established. The first parameter is the **single-pass methane conversion** expressed in **Eq. 1**.

$$X_{CH_4} = \frac{\text{mol } CH_{4,in} - \text{mol } CH_{4,out}}{\text{mol } CH_{4,in}} \times 100\% \quad \text{Eq. 1}$$

The second parameter is **benzene yield**, given that benzene is the main product with the highest selectivity, and it is calculated as the carbon moles of benzene divided by the carbon moles of methane fed into the reactor according to Jeong et al. (2020)'s definition, it is expressed in **Eq. 2**

$$Y_{C_6H_6} = \frac{6 \times \text{mol } C_6H_6}{\text{mol } CH_{4,in}} \times 100\% \quad \text{Eq. 2}$$

The third and final parameter is the **negative Deactivation slope (D-slope)** which represents the amount of the deactivation in the first reaction cycle, from the start of the induction period at

TOS_{SI} till the last reported methane conversion in the first cycle, so the conversion at TOS_{D3} . It is calculated as shown in Eq. 3.

The **D-Slope** has the unit of $(\Delta X_{CH_4}/h)$ and it represents a decrease in the conversion over time; for simplification, the negative of the slope was taken so it is easier to compare with positive values. The higher the value of the **D-slope**, the worst is the performance of the catalyst, as it indicates higher coke deposition, so a faster rate of deactivation. The lower the **D-slope**, the better the performance, which is an indication of catalytic stability during the first reaction cycle. It is also worth mentioning that the **D-slope** is a representation of the local performance and not the global performance after a separate regeneration step is applied.

$$\text{negative Deactivation slope} = \frac{-(X_{CH_4, TOS_{D3}} - X_{CH_4, TOS_{SI}})}{TOS_{D3} - TOS_{SI}} \quad \text{Eq. 3}$$

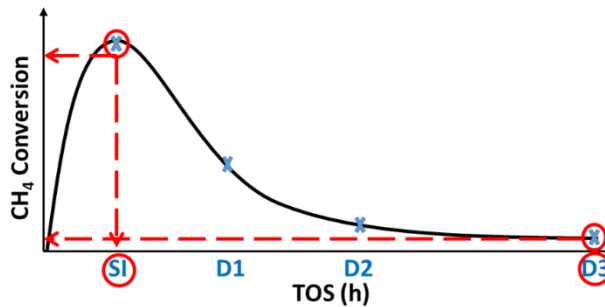


Figure 14: Calculating the D-Slope factor

5.3 Quantified Database Results and Discussion

Effect of Mo content and Si/Al ratio

Mo content is a very important factor in the MDA process, considering that Mo carbide is the active site that helps initiate the chain of reactions by breaking the C-H bond. Increasing the Mo content increases, the methane conversion, which also increases the coke formation leading to a more severe deactivation. Therefore, it is important to find the optimum Mo content added to the zeolite, leading to the highest methane conversion while achieving good product selectivity and yield. Several groups studied the effect of Mo content on the catalyst performance. Han et al. (2019) tested a range of Mo content between 1-7 wt% and the maximum benzene yield after 10h of reaction time was achieved with Mo of 5 wt%, while the effect of the Mo content on methane conversion was not as significant for Mo content of 5-7 wt%. However, the study indicates that the optimum Mo content is 5 wt% due to the high accessibility of the active metal site Mo_2C and Brønsted acid sites in the zeolite microchannels. This was supported by Qi & Yang (2004), who tested a range of Mo content between 3 wt% and 9 wt% and the optimum Mo load was 6 wt%, which allowed the maximum methane conversion and benzene selectivity. However, others reported different results for the optimum Mo content. Tessonnier et al. (2008) found the optimum Mo content to be 2 wt%. The conflicting results highlighted the probability of having another factor that causes this inconclusive relation between Mo content and the catalytic performance. Many researchers started investigating this and found that the structure of zeolites, consisting of Si, Al, and O, with different Si/Al ratio, might affect the performance. Tessonnier et al. (2008) tested this theory by synthesizing two types of zeolites with different Si/Al ratios and found that

for a catalyst with a higher Si/Al ratio of about 45, the 2wt%Mo resulted in better results than 4wt%. While for lower Si/Al ratio, typically around 15, 4wt%Mo resulted in more stable performance and higher conversion and yield throughout the reaction. This aligns with what Z.R. Ismagilov et al. (2017) reported. This group also suggested that using a smaller Si/Al ratio is better as it allows higher Mo content, which increases the activity of the catalyst. Whereas, when using zeolite with a higher Si/Al ratio, higher the Mo content leads to more coke content and faster deactivation.

The relation between Mo content and Si/Al ratio can be explained by the anchoring mode of Mo after impregnation. At a higher Si/Al ratio (mostly greater than 40), Mo dimers (Mo_2O_5) predominantly form, and some monomers might form as well. However, Mo monomers are less stable at higher ratios. When Mo dimers form, it is believed that they can only catalyze coke formation under MDA reaction conditions (Tessonier et al., 2008). Furthermore, the catalytic activity is higher when Mo anchoring mode is monomeric, which leads to the lowest coke deposition on the surface of the catalyst as opposed to inside the catalyst pores. Therefore, lower Mo content (2 wt%) is preferred for zeolites with a higher Si/Al ratio because if the amount of Mo is increased, this will promote conversion to coke rather than benzene. Higher Mo content (4.5-6 wt%) leads to better results for zeolites with a lower Si/Al ratio because the higher the Mo content, the greater the catalytic activity, which enhances methane conversion to benzene until a certain limit, then the amount of coke formed is too high that it covers the external surface and block the catalyst pores stopping the reaction.

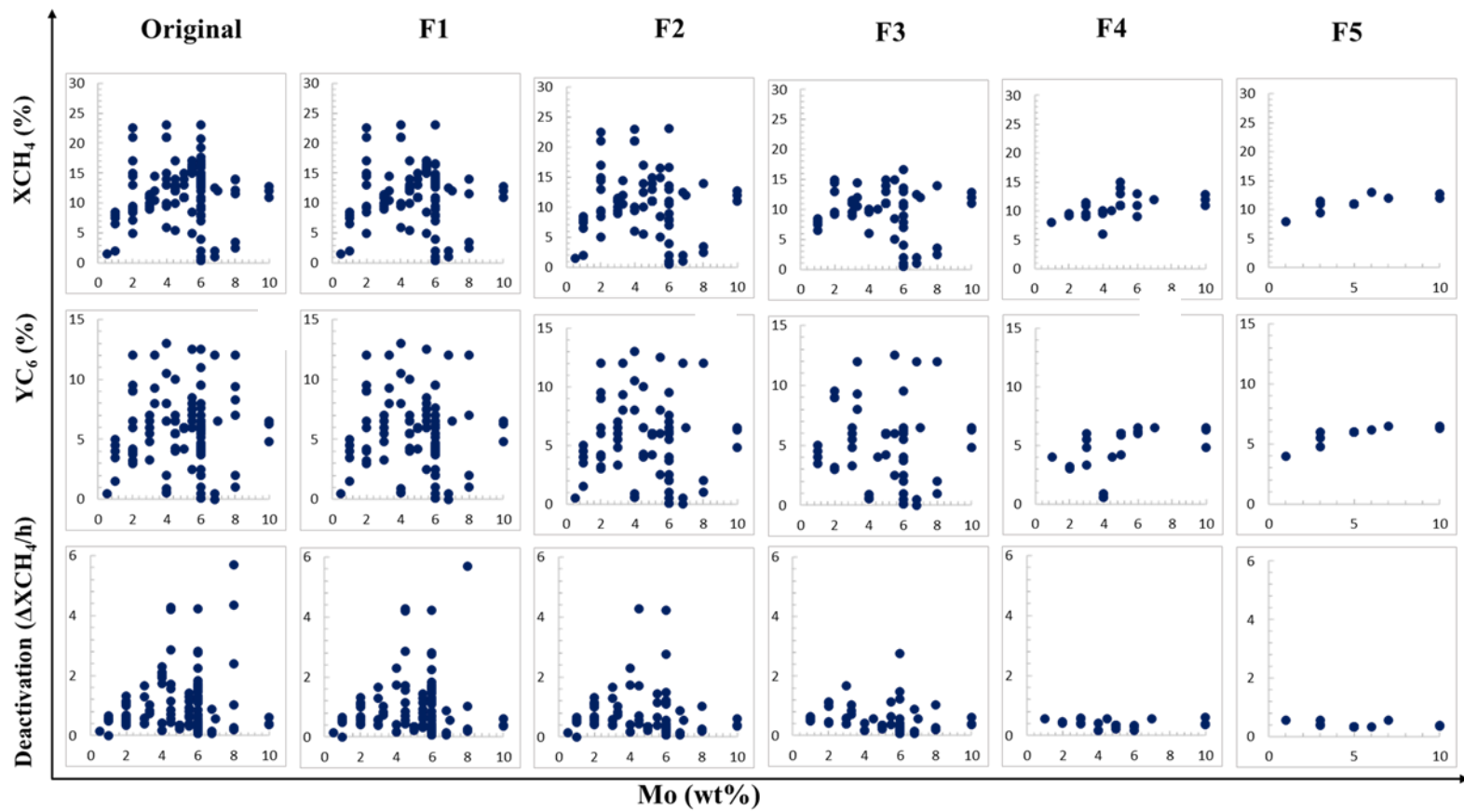


Figure 15: Effect of Mo content on methane conversion, benzene yield, and the D-Slope

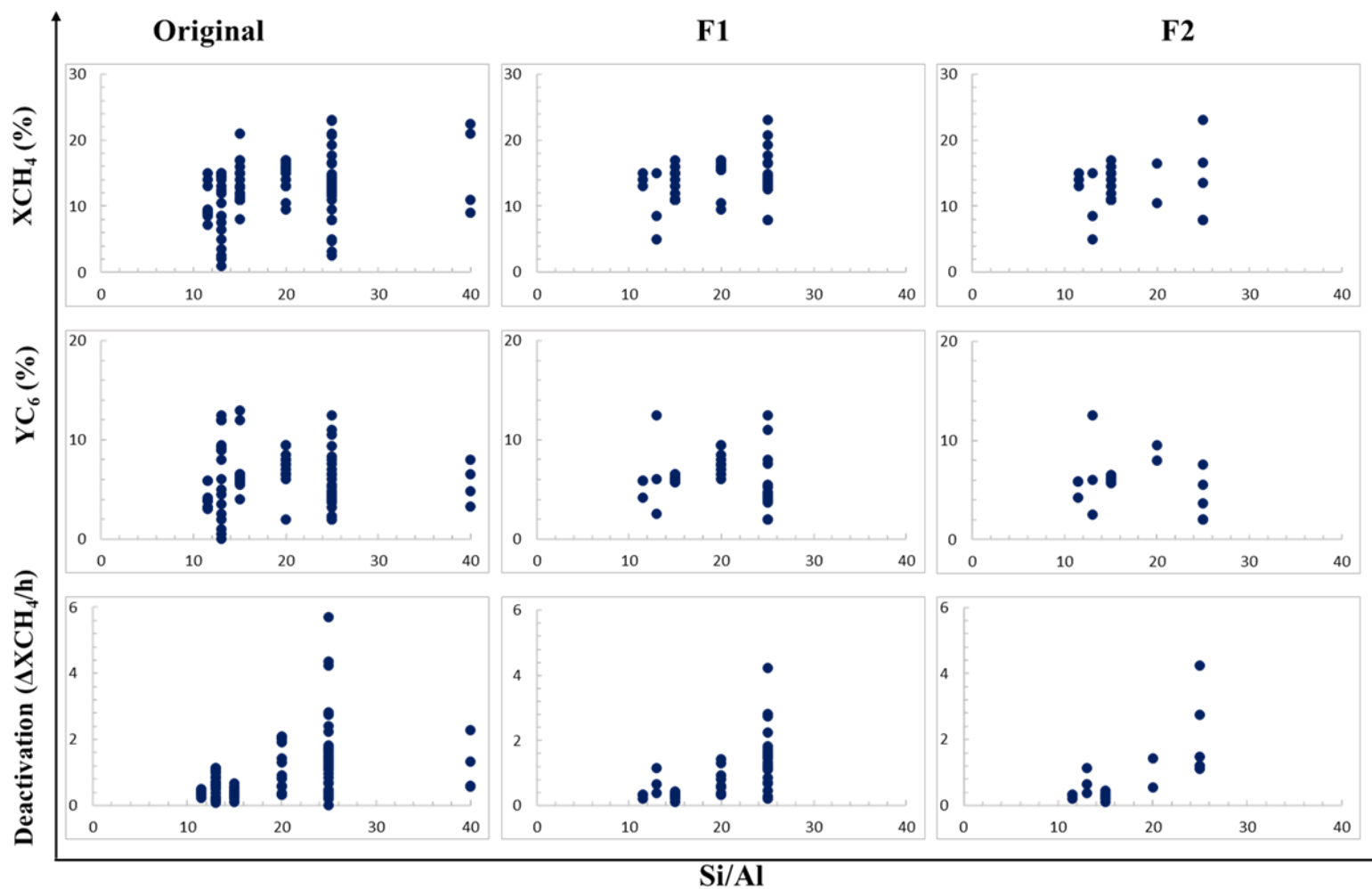


Figure 16: Effect of Si/Al ratio on methane conversion, benzene yield, and the D-Slope

To test the claimed hypothesis in the literature, several figures were created from the quantified database to verify the effect of Mo content and its relation to Si/Al ratio. The first set of figures “original” in **Figure 15** are of all the data points from studies that used Mo metal as part of its catalyst. The figures represent Mo content against methane conversion, benzene yield, and the **D-Slope**. As can be seen, no clear conclusion or trend can be interpreted from these figures. Then the data points were filtered “F1” to include only Mo/HZSM-5 catalyst, excluding Mo/HMCM-22, Mo/TNU, Mo/IM-5, and more. Then, a second filter was applied, “F2” which included only data points of studies that used Mo as the only metal without the addition of another metal and used continuous feed of methane only. A third filter, “F3” in **Figure 15**, was fixing one reaction temperature at 700°C. A fourth filter was then applied “F4” to fix a range of space velocity from 750 up to 1500 ml/g_{cat}/h. A clear trend was not observed for the methane conversion and the benzene yield plots; however, it can be clearly seen that for the lower space velocity range that was selected, the **D-Slope** is noticeably lower, with a maximum value of 0.6, compared to the “original” plot, which included studies with **D-Slope** of 6. This means that higher space velocities have a great negative impact on catalyst stability. Following that, a fifth filter was applied, “F5” to select a range of Si/Al ratio between 15-25. There is somewhat of a clear trend that the conversion increases as the Mo content increases until around 7wt%, then the conversion starts to decrease. As for the benzene yield, the results are not as conclusive given that not all the studies report this value; however, it can still be seen that the higher the Mo content, the higher the benzene yield, until about 4wt%. For higher Mo content, the benzene yield is somewhat stable. Observing the plot for the **D-Slope**, it does not show a clear trend, with the lowest value being 0.3, which was

reported at 5 and 6wt%. This shows that the claim about the Mo content affecting the deactivation rate is not valid for all reaction conditions.

It can be seen from the plots above **Figure 16** that from the “original” plot, the Si/Al ratio for Mo/HZSM-5 catalyst can range between 11-40. The original figures include data points for Mo/HZSM-5 catalyst only. The first filter applied “F1” was for the Mo content, which included Mo content between 5-6 wt%, which is the most commonly used composition in literature. No conclusion can be drawn from these figures as the performance varies significantly for each Si/Al ratio value. However, it can be seen that in literature, the Si/Al ratio commonly used for such Mo content is between 11-25, with only one or two outliers. Then a second filter was added, “F2” to include only continuous methane feed; however, it did not give much more clarity on the effect of the Si/Al ratio. This means that the correlation between Si/Al ratio, methane conversion, and benzene yield that is claimed in literature may not be strong enough compared to other operating conditions. It is worth mentioning that the studies performed with a zeolite with a Si/Al ratio higher than 20 tend to have a higher **D-Slope**, which means that there could be a relation between the catalyst stability and the Si/Al ratio of the zeolite.

Effect of reaction temperature

To determine the effect of reaction temperature on the catalyst performance, different studies provided how different catalysts performed under different ranges of reaction temperatures. Skutil & Taniewski (2006) studied the effect of varying the reaction temperature within the range of 700-800°C over Mo/HZSM-5. The results showed that a reaction temperature of 800°C is too high for the MDA reaction; although it leads to the maximum initial methane conversion, it is not appropriate for the stability of the catalyst as it leads to extremely rapid deactivation. The optimum reaction temperature, according to this study, is 725°C. The work of Yuebing Xu et al. (2013), however, showed that when using Mo/HZSM-5 catalyst and a CH₄-H₂ periodic switch of 5min – 10min and testing for a reaction temperature range between 800 and 900°C, the optimum reaction temperature is 800°C. This study found the same trend as expected activity and stability, where a higher temperature leads to higher activity and lower catalytic stability. This study also showed that the benzene formation rate increases with increased temperature while its selectivity remains the same after 850°C. As for Naphthalene, the formation rate and selectivity reach their maximum at 800°C, then they both start decreasing. The optimum reaction temperature was selected based on the coke formation rate and the catalyst stability. At 800°C, the coke formation rate is lowest, and the coke accumulated during the reaction period is the smallest among the temperature range. Additionally, the methane conversion, benzene formation rate, and benzene selectivity remained almost the same for 2h of reaction time at 800°C. A reaction temperature of 900°C did not last for longer than 25mins then the catalyst dies, and the coke accumulated is irreversible under the switch conditions. This study also investigated the possibility of the high reaction temperature affecting the catalyst structure. It was found through XRD analysis that the structure of the catalyst remained

unchanged over the entire temperature range, which means that the instability of the catalyst at higher temperatures is solely due to the rapid accumulation of coke on the surface of the catalyst, preventing the reactant CH_4 from accessing the active sites located inside the catalyst pores.

The work done by Dutta et al. (2018) confirmed the thermodynamics of the MDA reaction by testing the reaction over GaN catalyst for a temperature range between 200°C and 600°C and showed that methane conversion begins at a temperature above 500°C , while benzene formation starts at a temperature above 600°C . Then the optimum reaction temperature was determined when testing a temperature range of $650 - 710^\circ\text{C}$. The optimum temperature was found to be 710°C , where the maximum methane conversion, benzene, and hydrogen formation rates were achieved. It is important to point out that the induction period was not affected by the reaction temperature, according to this study.

The work of Abedin et al. (2020) focused on testing the reaction over Mo-SH catalyst for a temperature range of $600-700^\circ\text{C}$. The reaction was tested for 15 hours, during which methane conversion decreased rapidly for the higher temperature in the testing range (700°C) during the first 5h of the reaction and then maintained its stability for the remaining 10h. Whereas for 650°C reaction temperature, the conversion gradually decreased for about 10h but then became steady at low conversion for the last 5h of reaction time. However, for a reaction temperature of 600°C , although the lowest maximum conversion is achieved, the conversion is maintained for about 8h of the reaction time. The author also tested the effect of the different temperatures on benzene and ethylene selectivity. The results showed that the benzene selectivity over this specific catalyst decreases gradually over the entire reaction time, but for 700°C , the benzene selectivity falls to 0% after only 9h of reaction time. However, the ethylene selectivity gradually increases over the

reaction time for all reaction temperatures, showing that this catalyst is more suitable for olefin production processes rather than MDA reaction. The work of Lasobras et al. (2019) tested different parameters that influence the MDA reaction, which included a study on the reaction temperature. The reaction took place in a fluidized bed, and the catalyst used is Mo/HZSM-5/bentonite. The temperature range chosen was 675 - 725°C, and the optimum reaction temperature was selected based on maximizing methane conversion and benzene selectivity. This work showed that the conversion at a reaction temperature of 600°C is lower than that at 700°C; however, when the temperature is increased to 725°C, the conversion remains the same. The author believes that the reason for that is that the coke formation reaction is favored at higher temperatures causing the catalyst to deactivate and decreasing the expected conversion. Due to that same reason, the selectivity of benzene at 725°C was lower than that at 700°C. Therefore, the optimum temperature for the MDA reaction was assumed to be 700°C.

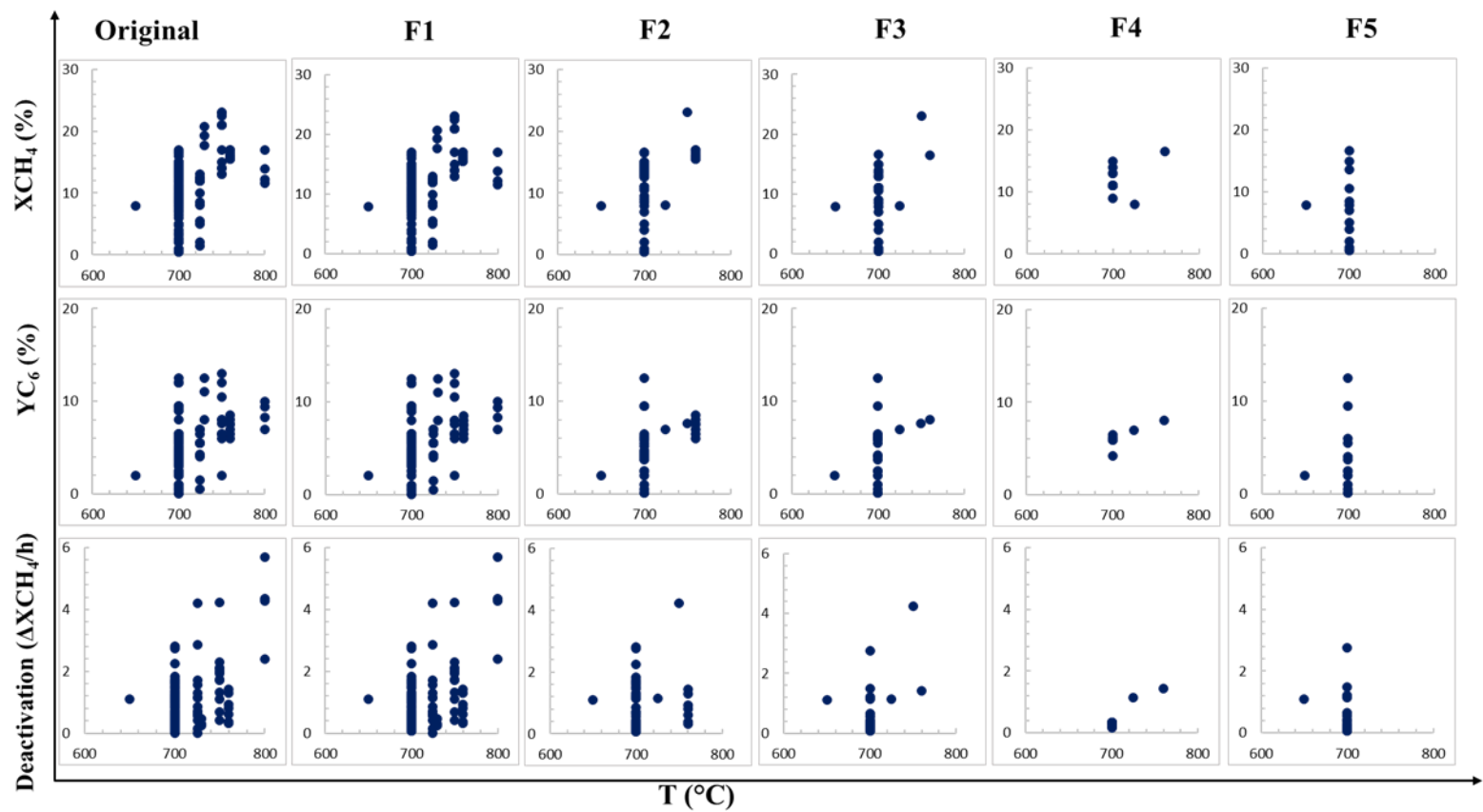


Figure 17: Effect of reaction temperature on methane conversion, benzene yield, and the D-Slope

Figure 17 presents data points from the quantified database of pseudo-steady-state methane conversion and benzene yield and the **D-Slope** over the total time on stream at different reaction temperatures. The first plot in **Figure 17**, “original” is of all the data points, shows that the temperature range investigated in the literature is between 650°C and 800°C; however, it does not show any trend. It is important to note that the increase in reaction temperature should lead to higher conversion, according to thermodynamics. For example, experiments performed at 700°C should result in higher methane conversion than the ones carried out at 650°C. It can be seen from the data that the points that do not follow the thermodynamic rule have lower Mo content, which highlights the great impact of Mo content on the performance.

The first filter that was applied, “F1” is the catalyst Mo/HZSM-5. The second filter, “F2”, is the metal composition between 5-6 Mo wt%. The third “F3” in **Figure 17** is the feeding mode, selected to be a continuous feed of only methane. The fourth filter, “F4” is the space velocity, including space velocities between 750 and 1550 (ml/g_{cat}/h), which is the range most commonly applied for the MDA process. Although there was no conclusion from the figures after the first three filters, a conclusion can be drawn from the results of the fourth filter. The **D-Slope** plot can confirm one of the claims that the higher reaction temperatures lead to faster deactivation, which is represented in higher **D-Slope** values. However, when a fifth filter was added “F5”, which is for a higher space velocity range (higher than 1550 (ml/g_{cat}/h), the conclusion regarding the deactivation rate increasing as the temperature increases is no longer valid given that most of the data points are at a temperature of 700°C, and the corresponding conversion, yield, and **D-Slope** values vary significantly. Therefore, it must be due to other factors such as Si/Al ratio, particle size, or preparation method.

Effect of space velocity

The effect of space velocity on the MDA reaction is studied, as shown in **Figure 18**. The effect of space velocity on the reaction outcomes is connected to the particle size, which is related to the impact of external mass transfer. However, it should be mentioned that there are very limited studies that investigated this relation between particle size and space velocity, and they tested for particle size between (0.2-4 μm). While most of the MDA reaction studies use a catalyst with a relatively large particle size in the range of (150-850 μm). With that in mind, some general conclusions can be drawn from the literature about the effect of space velocity on the MDA reaction. Studies done by Skutil & Taniewski (2006), Abedin et al. (2020), and Jeong et al. (2020) showed that a greater space velocity leads to a decrease in the maximum conversion that can be achieved by the catalyst, benzene selectivity, and total amount of coke formed along with a shorter induction period. It is worth mentioning that the range of space velocities that have been studied for the MDA reaction is very large. It can go as low as 750 ml/g/h up to 60,000 ml/g/h. Nevertheless, at space velocities higher than 5000 ml/g/h, the maximum achievable methane conversion is very low. Therefore, when referring to higher space velocity, it is mostly in the range of 3000-5000 ml/g/h for a regular size catalyst in the order of 100 to a couple of 100s μm . While for very small particles, in the order of 1-10 μm , a high space velocity is probably greater than 12000 ml/g/h.

When the reaction is performed at higher space velocities with a particle size (150-850 μm), the rate-determining step might change from the catalytic formation of aromatics to their diffusion out of the zeolite channels. To avoid such internal diffusion limitations, C. Sun et al.

(2015) found that having smaller channels should be used and has a positive effect on the long-term life of the catalyst even at low space velocities.

Abedin et al. (2020) found that using a smaller particle size can prevent the decrease in benzene concentration/selectivity at higher space velocities while selectively producing less coke; however, there still is a fast deactivation challenge for which an appropriate regeneration strategy should be used. A small zeolite particles-based catalyst, when compared with those based on large HZSM-5 particles, has a large number of short zeolitic channels and little diffusion resistance, which surely allows a simultaneous exposure of a large number of inside active sites to the reactant methane, reaction intermediates and formed aromatics at a specific time of the reaction. Based on the above conclusions, it can be inferred that a balance between the particle size and space velocity needs to be found to maintain methane conversion and benzene selectivity at appropriate ranges while limiting the coke formation and maintaining a smaller induction period.

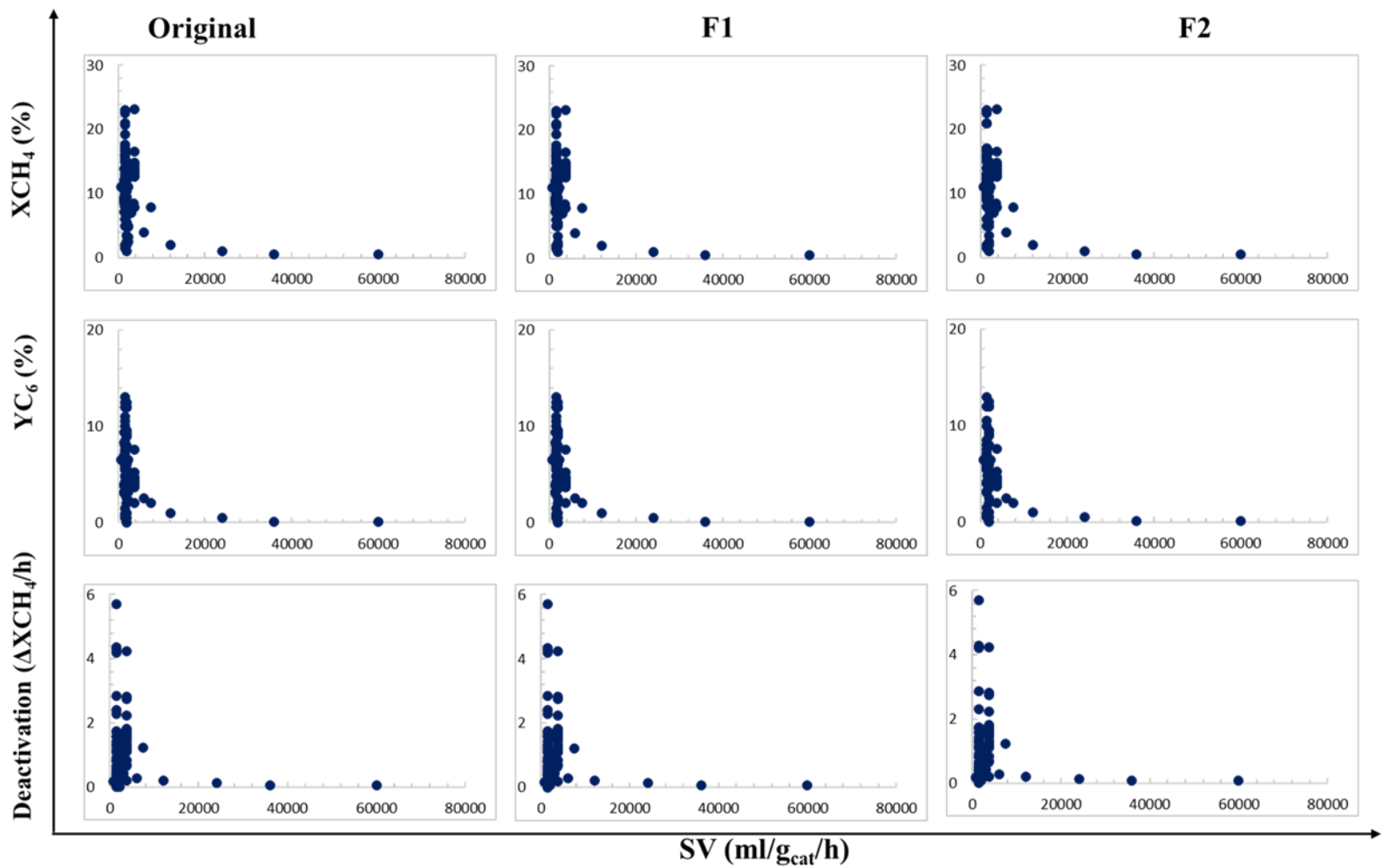


Figure 18: Effect of space velocity on methane conversion, benzene yield, and the D-Slope

The above **Figure 18** was plotted for the methane conversion, benzene yield, and **D-slope** at different space velocities. The first figure is plotted “original” for all the data points in the database that report methane conversion. The only conclusion that can be seen from these original plots is that most studies focus on selecting a very low space velocity value. The first filter that was applied, “F1” was for the catalyst type, which was chosen to be Mo/HZSM-5. The second “F2” was the metal composition which included results from experiments using Mo as the only metal in the catalyst. It can be seen that most of the experiments were performed at space velocity lower than 2000 ml/g/h, and the only conclusion that can be seen is that at very high space velocity, the methane conversion and the benzene yield decrease gradually. The main reason for that is that the residence time of the feed inside the catalyst bed decreases, causing the majority of feed gas to leave before the reaction can take place. However, the rule does not apply at smaller ranges, as is clear from the plots. Other filters were applied, but no trends or correlations, indicating that space velocity might not have a strong affect.

Table 3: List of filters applied to the database for each variable

Mo content (Figure 15)	
Original	All data points
F1	Catalyst type (Mo/HZSM-5)
F2	Metal composition (Mo) and feeding mode- continuous CH ₄
F3	Reaction temperature (700°C)
F4	SV (up to 1550ml/g _{cat} /h)
F5	Si/Al ratio (12-25)
Si/Al ratio (Figure 16)	
Original	Catalyst type (Mo/HZSM-5)
F1	Mo content (5-6)
F2	Feeding mode-continuous CH ₄
Reaction temperature (Figure 17)	
Original	All data points
F1	Catalyst type (Mo/HZSM-5)
F2	Metal composition (Mo)
F3	Feeding mode
F4	SV (up to 1550 ml/g _{cat} /h)
F5	SV (higher than 1550 ml/g _{cat} /h)
Space velocity (Figure 18)	
Original	All data points
F1	Catalyst type (Mo/HZSM-5)
F2	Metal composition (Mo)

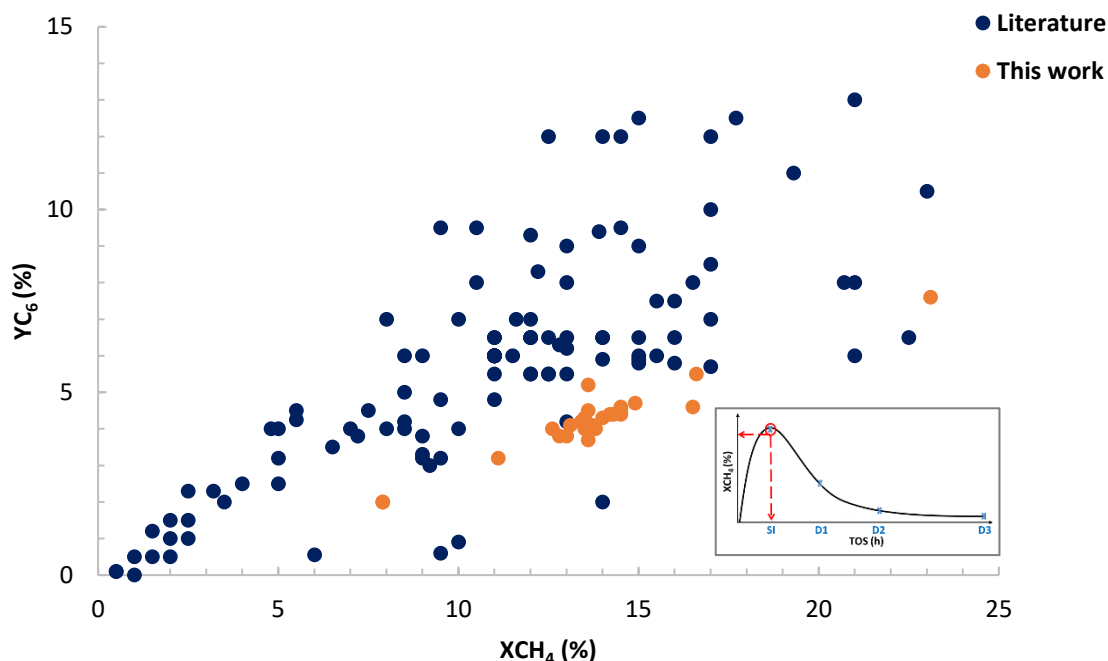


Figure 19: The effect of the change in methane conversion on the benzene yield at pseudo-steady-state

Other plots were generated from the quantified database to guide future experiments in this field and verify the experimental work done in this study. **Figure 19** shows how the change in the methane conversion at the pseudo-steady-state influenced the benzene yield. Such a plot helps to identify the appropriate operating conditions from literature and the least applicable ones.

Firstly, it can be seen that the experimental work done in this study is comparable to that in literature, which gives confidence in the experimental results produced.

After identifying the highest performances from the figure, it is important to mention the conditions that lead to that performance. One of the highest performances was obtained by co-feeding O₂; however, this study used a unique catalyst that consisted of Sr and La metals on top of the Mo/HZSM-5 catalyst, which could be the main factor for the performance. This study had a

D-Slope of 1.1 represents good stability; however, it is not the best, given that other studies had a **D-Slope** of less than 0.1. Another very notable performance was demonstrated by a study that added very small amounts of CH_3OH to the feed, attempting to couple methylation reaction with the MDA reaction. This study showed high initial activity and a **D-Slope** of 0.8. However, the benzene yield decreased significantly over time. These results show the significance of the **D-Slope**; however, they also highlight the need for a factor that represents the benzene yield over the entire reaction time.

As a result, another factor was created to indicate the total production of benzene over the total reaction time, which is referred to as **Global YC_6** . This factor can be best explained in **Figure 20**.

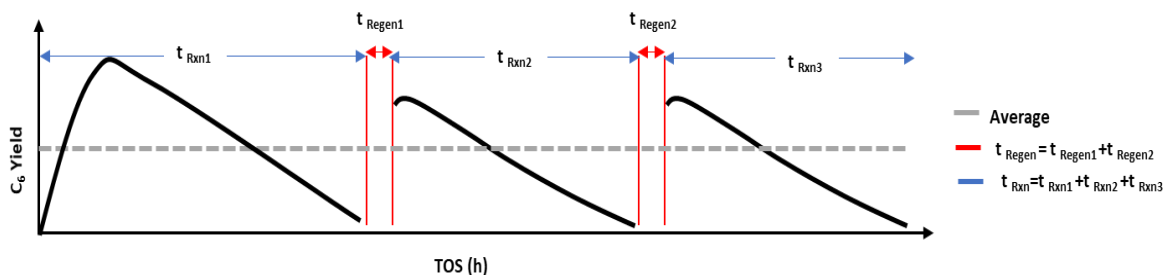


Figure 20: Global YC_6 illustration

The factor considers an average benzene yield value over the entire total time on stream (TOS). However, as can be seen from **Figure 20**, this includes the regeneration time. Thus, we multiplied this average yield by a time factor to eliminate the time needed for regeneration. This factor, which is the ratio between the reaction times only divided by the total TOS, is shown in **Eq. 4**. The time factor helps indicate which conditions maximize the total benzene production for a more cost-efficient process.

$$\text{Global } YC_6 = \text{Average } YC_6 \times \frac{\sum t_{Rxn}}{TOS} \quad \text{Eq. 4}$$

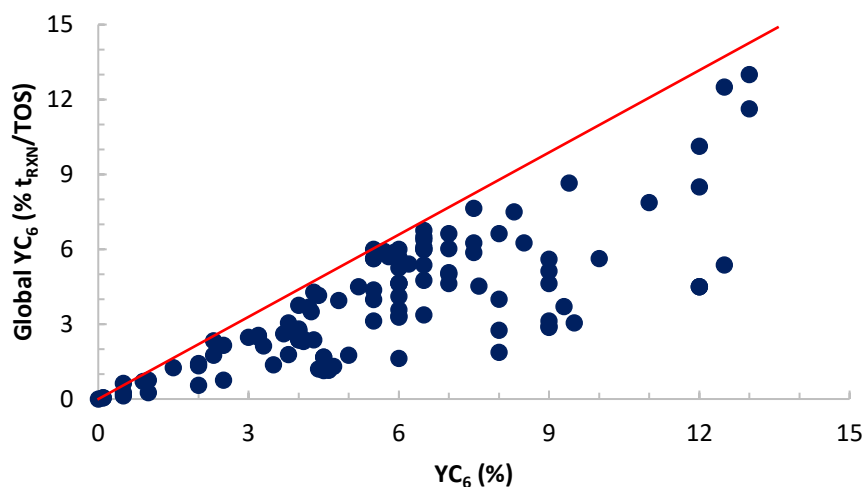


Figure 21: The effect of varying YC_6 on Global YC_6

The above **Figure 21** shows how the **Global YC_6** factor (y-axis) varies as the pseudo-steady-state benzene yield for the first cycle (x-axis) changes. The better the performance, the higher the benzene yield and the higher the **Global YC_6** factor. The trend that can be seen from this figure shows that the increase in the benzene yield at steady-state corresponds to a higher **Global YC_6** . This may indicate that a high initial activity could result in more stable performance, therefore, higher production.

Some of the studies achieved high values for both the initial yield and the **Global YC_6** using continuous feeding of CO_2 in their feed and added Mg to the Mo/HZSM-5 catalyst. Another study added minor amounts of C_2H_4 and C_2H_6 to the feed.

6. EXPERIMENTAL STUDIES

This work consists of multiple experimental studies. The first aims to validate that the experimental setup is operational by replicating a selected literature work. The second and third sections include periodic switch and pulse feeding experiments. Two regenerating molecules were selected for these studies. The first is H₂, which will perform the function of reductive regeneration. The second molecule is CO₂ which is an oxidative regeneration.

6.1 Experimental Setup

The experimental studies performed in this work were done in the Catalytic Reactor Laboratory using the YaraCat testing setup **Figure 22**.

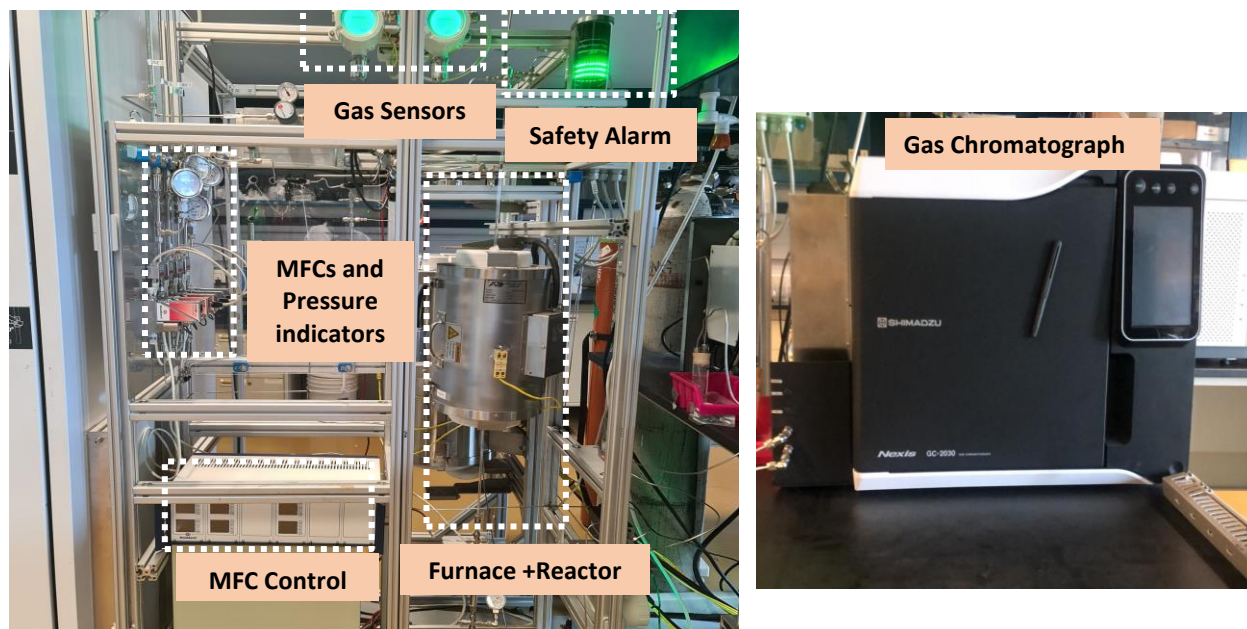


Figure 22: YaraCat testing setup

The setup consists of the following equipment:

Mass flow control system

The gases connected to the setup are controlled through a mass flow control system and mass flow control unit. These gases are:

- Carbon dioxide (99.995%)
- Methane (95%/ 5% Ar)
- Hydrogen (99.999%)
- Argon (99.999%)

The gas cylinders were purchased from the local vendor Buzwair.

All the gas cylinders are stored in gas cabinets; the gas lines are extended from inside the gas cabinets to the mass flow controllers, which control the flow rate for each gas line separately, as seen in **Figure 23**.

Furnace and reactor system

The gas passes through the mass flow control system into the reactor system. This system consists of a quartz reactor with a 4mm inner diameter inserted inside a furnace. The furnace is connected to a temperature controller. Both are purchased from Applied Test Systems (ATS). The furnace can handle temperatures up to 1200°C. The furnace temperature is controlled via the temperature controller. After the gas leaves the reactor, it enters the Gas Chromatograph (GC) analysis unit, explained in more detail in **Section 7.3**.



Figure 23: Mass flow controllers and pressure indicators



Figure 24: Temperature controller

Safety and Alarm system

A safety system was installed into the setup to monitor any gas leakage. Four gas sensors are installed for: methane, carbon monoxide, carbon dioxide, and heavy hydrocarbons (C8+). The alarm system is connected to the gas detectors and will send visual signals in the case of a gas leak. The alarm system gives a green signal by default. If a leak is detected, the green light will change to yellow or red depending on the concentration detected.



Figure 25: Safety alarm system

All the gas detectors need to be annually calibrated to ensure a safe operation and accurate measurements.

Data analysis through Gas Chromatograph (GC)

Gas Chromatography is a widely used analysis tool for analyzing reaction products. It is a technique of separation of a gas mixture into its components to identify their compositions and concentration. The output of a chromatograph can be a graph of a detector's output, information about the heights of the different peaks and their areas, as well as identifying the molecules based on their molecular weights (Blumberg, 2012). The GC used in this work was equipped with Thermal Conductivity Detector (TCD), a non-destructive and concentration-sensitive detector. It differentiates molecules based on their thermal conductivities. This is a universal detector and is used for the detection of organic and non-organic molecules. The second detector is the Flame Ionization Detector (FID), and it is a mass-sensitive detector that detects compounds based on their

masses. This detector uses hydrogen flame to combust organic compounds (Klee, 2012). The GC results are represented as the retention time vs. the number of gasses absorbed or present.

The GC used in this work is Nexis GC-2030 from Shimadzu. This GC has two TCD detectors; TCD1 detects light hydrocarbons, as well as; Argon, Oxygen, Carbon dioxide, and Carbon monoxide. While TCD2 detects Hydrogen and Helium. The carrier gases used for these detectors are Helium and Nitrogen, respectively. The GC is also equipped with two FID detectors, FID1 detects light hydrocarbons, while FID2 detects heavier hydrocarbons (C6+). The carrier gas for both FID is Hydrogen. The GC is also connected to a Zero air gas cylinder required for the opening and closing of the valves.



Figure 26: Gas Chromatograph (Adapted from Nexis GC-2030 : SHIMADZU (Shimadzu Corporation), n.d.)

The performance of the GC is continuously monitored to ensure accurate and stable results.

Data analysis through Thermogravimetric analysis (TGA)

Thermogravimetric analysis (TGA) is an experimental technique to measure the change in sample mass versus temperature and/or time in a controlled atmosphere. The TGA analysis was used to quantify the amount of coke accumulated on the catalyst during the reaction period. The gas used during the ramping in the TGA for this reaction is air as it includes oxygen which will react with the coke and burn it, which will appear as a percentage loss in the sample weight.

6.2 Experimental Procedure

This section will include a detailed explanation of the general experimental procedure followed to perform any experiment in this work starting with the preparation of the catalyst, loading the reactor, connecting the MFC system, starting the GC, and unloading the catalyst.

Catalyst preparation

The catalyst used in all these experiments is Mo/HZSM-5, prepared using an incipient wetness preparation method where Mo metal was impregnated into a zeolite base (HZSM-5). This catalyst was prepared and provided by TOTAL. The Mo content in the final catalyst is 6wt%. The only treatment applied to the received catalyst calcination at 500°C for 4h with a heating rate of 10°C/min. The desired particle size of the catalyst is 300-425µm; therefore, the catalyst was first pelletized to obtain the desired size.

To pelletize the catalyst, a circular die of diameter 15mm and 40mm depth was used. First, the die sleeve is added to the bottom of the mold, and the mold is inserted. Second, the catalyst in the powder form is added, and the die sleeve is used to secure it in place.

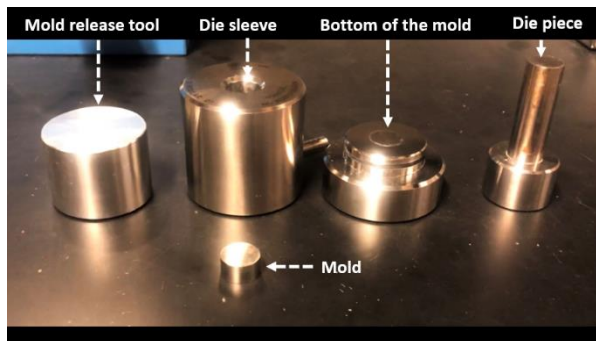


Figure 27: Circular die used to create a pellet

The die is then transferred to the pelletizing machine and is secured, and the machine is set to a pressure of 10 bars; the die was pressurized for about 2-3 minutes, then it was taken out, and the catalyst pellet was collected. The reason behind pelletizing the catalyst is to obtain and create a bigger particle size then crush it to the required size range.

After that, the pellet was carefully crushed using a mortar and a pestle, then sieved to the required particle size range of 300-425 μ m.



Figure 28: Pelletizing machine



Figure 29: Mortar and pestle



Figure 30: Sieves of sizes 300 and 425 μ m

Loading the reactor

The catalyst is then loaded into a quartz reactor of 4mm inner diameter. It is important to mention that this reaction is performed under isothermal conditions. Therefore, it is important to load the catalyst within the isothermal zone of the reactor when inserted in the furnace. The region was previously determined.

The reactor is purged with Air before it is used to remove any impurities, then the amount of catalyst required is weighed. The first step of loading the catalyst into the reactor is adding glass wool which is an inert, highly thermally isolating material to hold the catalyst in place. To load the reactor, it is fixed on a holder. Glass wool is packed into the reactor at the beginning of the isothermal zone. Then the catalyst is added, and another layer of glass wool is added to the top to hold the catalyst bed together. The reactor is then inserted into the furnace and fixed there. Then glass wool is added around the reactor to the top and bottom ends of the furnace for further isolation, as seen in **Figure 31**.



Figure 31: Loaded reactor inserted into the furnace

Pressure leak test

To ensure that the reactor is placed securely, a leak test is performed before each experiment by pressurizing the line with the connections attached to the reactor. This is done by pressuring the system at 1 bar using the backpressure regulator that is connected to the outlet of the reactor, which can be controlled from the MFC control unit mentioned previously. An inert gas (Ar) is used to perform the leak test so that in case there is a leak, an inert gas leaking into the atmosphere is not dangerous. The gas is fed into the reactor at a flow rate of 30ml/min, and the back-pressure regulator is set to 0.5 bar; once the line has been pressurized to the set pressure value, the flow of gas is stopped. The line is left pressurized for a few minutes while monitoring that the pressure stays the same. If the test is successful, the same process is repeated at 1 bar. In case the pressure goes down, a soap test is done around the connections that have been changed to detect where the location of the leak.

6.3 List of Performed Experimental Studies

Table 4: Experimental studies performed in this work

Study number	Study title	Objective	Results
1	Validation	Validate that our catalyst testing setup is working as expected by replicating an earlier study done in the literature	This work was validated with similar work from the literature
2	Reproducibility	Check the accuracy and the error margin of the final analysis by replicating the same test several times, each with a fresh catalyst.	The reproducibility of this work was confirmed, and an error margin was established
3	Pre-treatment conditions	Decide which pretreatment condition is needed for all upcoming tests in this work.	Pre-treating the gas in a CH ₄ -H ₂ gas mixture improved the performance and was selected for the remaining part of this work
4	Operating conditions	Testing different operating conditions to understand their effect on the process and fix them for future experiments	A space velocity of 3750 ml/g _{cat} /h and a reaction temperature of 700°C were selected for future experiments
5	Periodic feeding of H ₂ , CO ₂ , H ₂ +CO ₂	Changing the feed periodically from reaction to regeneration within a short period to enhance the performance	Introducing H ₂ in periodic switch mode was able to maintain a stable and good performance while introducing CO ₂ stopped the MDA reaction
6	Pulse feeding with H ₂ and CO ₂	Introducing the regenerating molecules in pulses frequently to test its effect on the process	Pulsing H ₂ frequently leads to good and stable performance, while pulsing CO ₂ shows a slight improvement to the performance but not to the stability of the process

6.3.1 Study 1: Validation – Replicating a Study in Literature

The first step in any experimental work is to ensure that the setup is performing well and the results are as expected and comparable to the literature. A study from literature was selected which used the same catalyst and operating conditions that can be achieved in the setup used in this work. The parameters applied can be seen in **Table 5**.

Table 5: Reaction conditions for study no. 1

Condition	Catalyst	Particle size	Ramping gas	Pressure	Temperature	Space velocity	Feed gas	Regeneration gas
Unit	-	μm	-	atm	$^{\circ}C$	$\frac{ml}{h \cdot g_{cat}}$	-	-
This work	6Mo/HZSM-5	300-425	H ₂ :CH ₄ 9:1	atmospheric	700	3750	5% Ar/ 95% CH ₄	H ₂
Literature	6Mo/HZSM-5	125-250	H ₂ :CH ₄ 9:1	atmospheric	700	1500	9% N ₂ / 91% CH ₄	H ₂

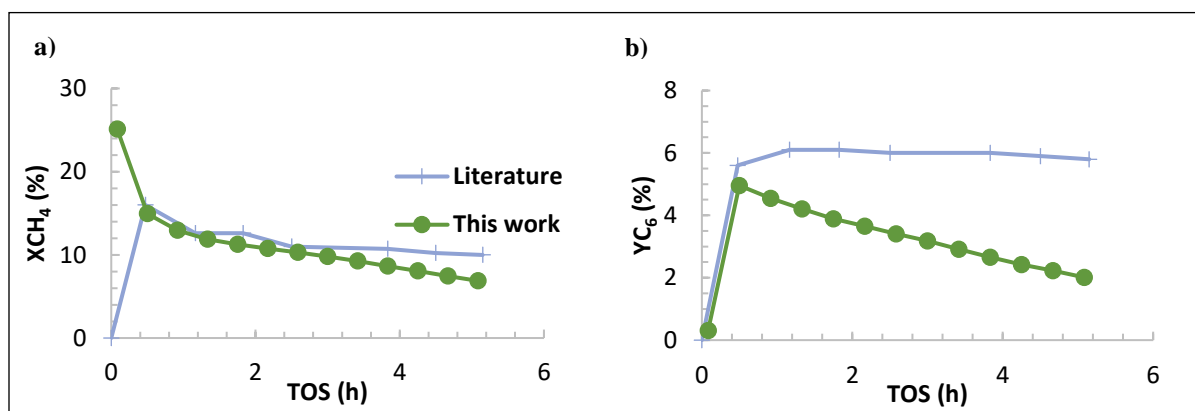


Figure 32: (a) CH₄ conversion (b) and C₆ yield of this work compared to literature

As shown in **Figure 32**, this work compares well with the selected work from the literature regarding methane conversion. It also has a similar C₆ yield. However, it deactivated faster. The only major differences between our work and the selected work from the literature are in the particle size and space velocity. According to claims in the literature, higher space velocity leads

to a higher deactivation rate, which is causing the deviation between the two results. Nonetheless, these results give confidence that the work done in this study is comparable and in agreement with the literature.

6.3.2 Study 2: Reproducibility

As part of the commissioning process to the setup, a baseline experiment was repeated four times to validate the setup and confirm its reproducibility, as well as to identify the error range. The experimental conditions were as mentioned in **Table 6** with a continuous methane flow for 3h, followed by 1h of regeneration with H₂, then another 3h of continuous methane flow to demonstrate the effect of the regeneration step.

Table 6: Reaction conditions for study no. 2

Condition	Catalyst	Particle size	Ramping gas	Pressure	Temperature	Space velocity	Feed gas	Regeneration gas
Unit	-	μm	-	atm	$^{\circ}\text{C}$	ml/g _{cat} /h	-	-
	6Mo/HZSM-5	300-425	H ₂ :CH ₄ 9:1	atmospheric	700	3750	5% Ar/ 95%CH ₄	H ₂

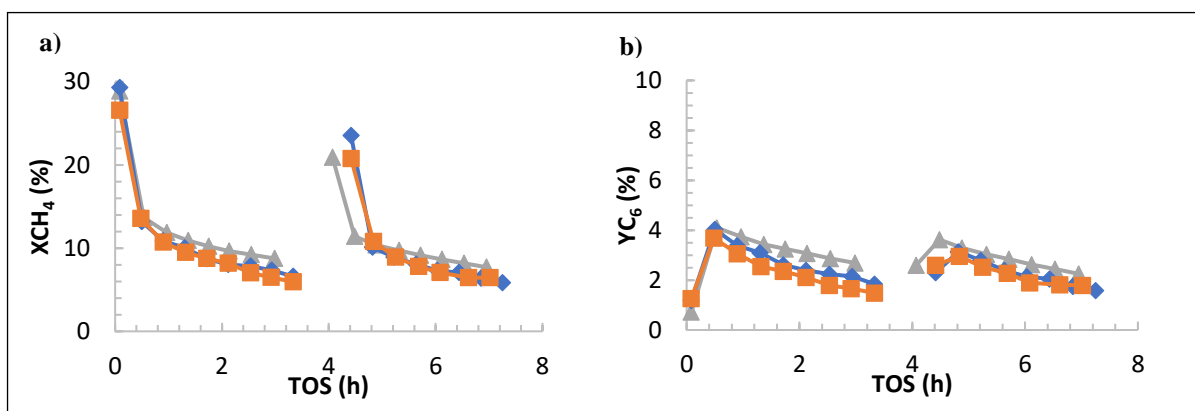


Figure 33: (a) CH₄ conversion (b) and C₆ yield of reproducibility studies

The general trend expected for the MDA reaction can be seen in **Figure 33**, with the methane conversion initially being very high during the induction period, as other reactions take place, such as the conversion of Mo-oxides to Mo₂C and coke formation. Then a decrease in the conversion is seen, indicating that deactivation started taking place. The same goes for the benzene yield that starts very low during the induction period, then reaches a maximum in the second data point taken at the beginning of the MDA reaction, followed by a decrease. After the regeneration period, the same trend can be seen, with an initial high activity indicating coke removal, followed by a decrease in performance when coke starts to accumulate once again. The above plots show good reproducibility in terms of methane conversion with about $\pm 2.2\%$. However, it seems that in the benzene yield, the error is much larger. Although the error is only around $\pm 1\%$, it is greater given that the range is between 0.5-4%.

6.3.3 Study 3: Pre-treatment Conditions

Another condition that was important to explore was the ramping gas or pre-treatment conditions. According to several studies, the pre-treatment conditions can have a significant effect on the catalyst performance. Some tried to pre-carburize the Mo-oxide sites to generate the active sites at lower temperatures to avoid the formation of coke during the induction period. This was achieved by introducing CH₄ in very small amounts alongside H₂ during ramping. This would help the formation of active sites while suppressing the MDA reaction and coke formation reaction thermodynamically by introducing excessive amounts of H₂.

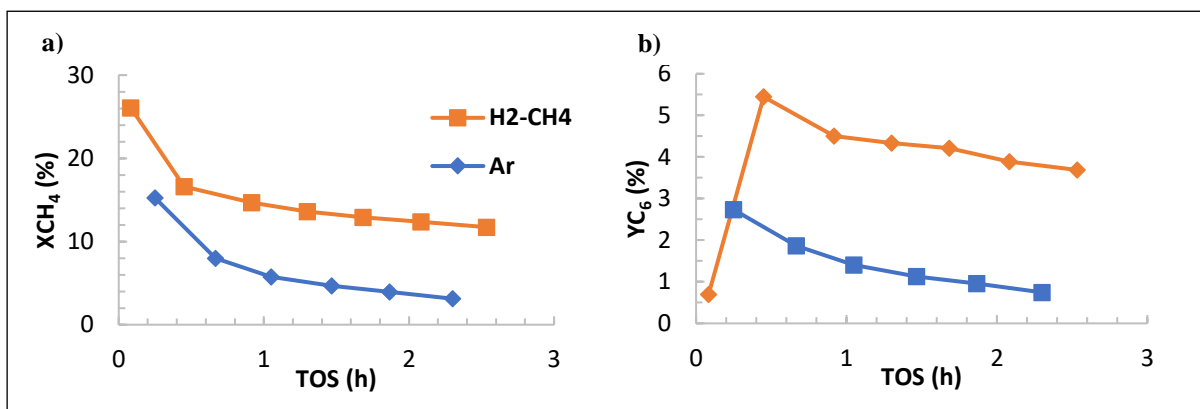


Figure 34: (a) CH₄ conversion (b) and C₆ yield for different pre-treatment conditions

Figure 34 shows the difference in performance when using pure Ar (an inert) during the ramping from room temperature to 700°C, and a gas mixture of H₂:CH₄ with 9:1 ratio. The results show an incredible increase in both the methane conversion and the benzene yield throughout about 2.5h of reaction. Therefore, the pre-treatment condition of H₂:CH₄ gas mixture with 9:1 ratio was applied during heating from room temperature to reaction temperature for all future experiments.

6.3.4 Study 4: Varying Operating Conditions

To find the most suitable operating conditions to perform the future experiments, a set of experiments were performed at different space velocities and reaction temperatures. This was also part of the commissioning process for the setup and to confirm that the results are somewhat comparable to the literature at different conditions.

i. Space Velocity

Space velocity is reportedly one of the most influential operating variables for the MDA reaction. The goal of this study was to confirm the effect of changing space velocity and select the

optimum value for future studies. The space velocity referred to in this study is the gas hourly space velocity, which represents the feed volumetric flow rate a gram of catalyst. The reaction space velocity can be changed by changing either the feed gas flow rate or the mass of the catalyst. In these studies, the volumetric flow rate of the feed gas was fixed, and the amount of catalyst was changed. The space velocities applied were 1875 ml/g_{cat}/h, 3750 ml/g_{cat}/h, and 7500 ml/g_{cat}/h and the mass of catalyst was 0.4, 0.2, and 0.1 respectively. The rest of the reaction conditions were as mentioned previously in **Table 6**.

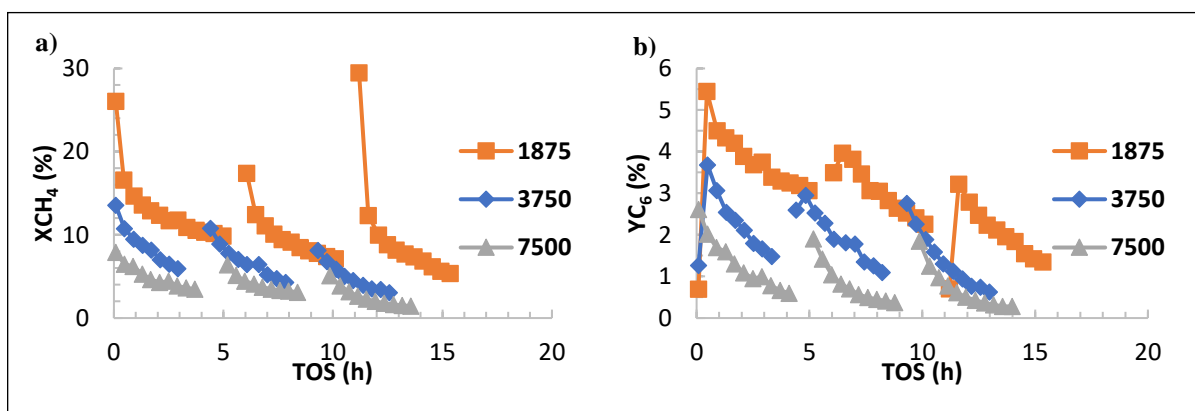


Figure 35: (a) CH₄ conversion (b) and C₆ yield for different space velocities

The results in **Figure 35** show that the lower the space velocity, the higher the methane conversion and the higher benzene yield. That is attributed to the effect of residence time given that at lower space velocity, the feed gas (CH₄) spends more time in the reactor, which affects the product distribution. In addition, the literature claims that the increase in space velocity leads to an increase in the deactivation rate, which was not observed from the above experiments. Looking at the **D-Slope** calculation, it can be seen that the slope varies from 1.3 for space velocity of 1875 ml/g_{cat}/h, 2.3 for space velocity of 3750 ml/g_{cat}/h, and 1.1 for space velocity of 7500 ml/g_{cat}/h.

The above results show that the lower the space velocity, the higher the performance. However, this might lead to internal mass transfer limitations. It is recommended to study the kinetics of the MDA reaction to identify where the mass transfer limitation lies to accurately decide the optimum reaction conditions. However, since such information was not mentioned clearly in the literature, a space velocity of 3750 ml/g_{cat}/h was selected for future studies.

ii. Reaction Temperature

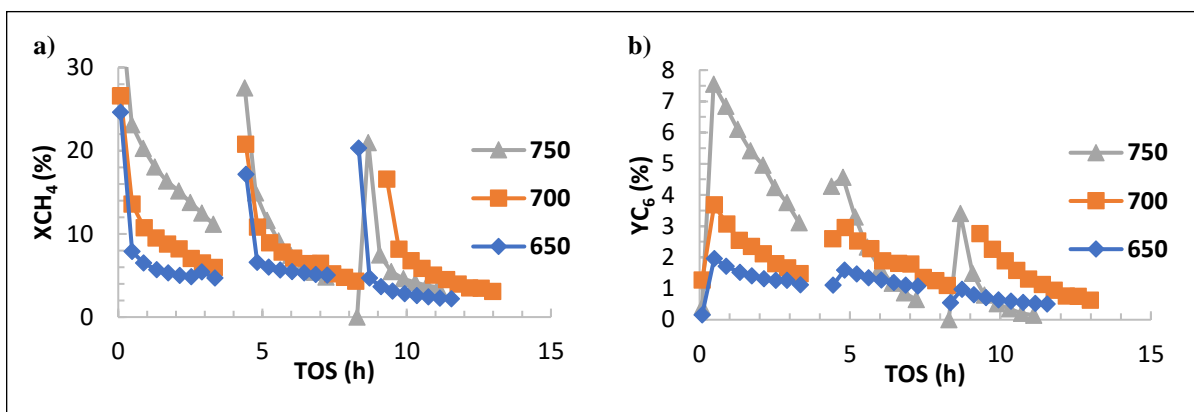


Figure 36: (a) CH₄ conversion (b) and C₆ yield for different reaction temperatures

The same conditions as mentioned in **Table 6** were applied for the above experiments. The space velocity of 3750 ml/g/h was selected from the previous study. The reaction and regeneration temperatures were varied for a total reaction time of about 14h with 2h of regeneration using H₂. The results shown in **Figure 36** compliance with thermodynamics as the temperature was increased, the initial activity is higher, which is clear from the methane conversion and the benzene yield. Another claim that was proved from these results was that the deactivation rate is accelerated when increasing the temperature. This could be observed by calculating the slope both locally and globally. The **D-Slope** values for the different experiments performed at 650, 700, and 750°C were

0.9, 2.3, 3.6, respectively. The temperature selected for the future experiments was 700°C, as it is one of the most commonly applied temperatures, allowing fair comparison between other studies.

Thermogravimetric analysis (TGA)

A sample of about 10mg was exposed to a fixed gas flow of 20 ml/min, air environment, and temperature ramping from room temperature to 800°C, at a rate of 10°C/min.

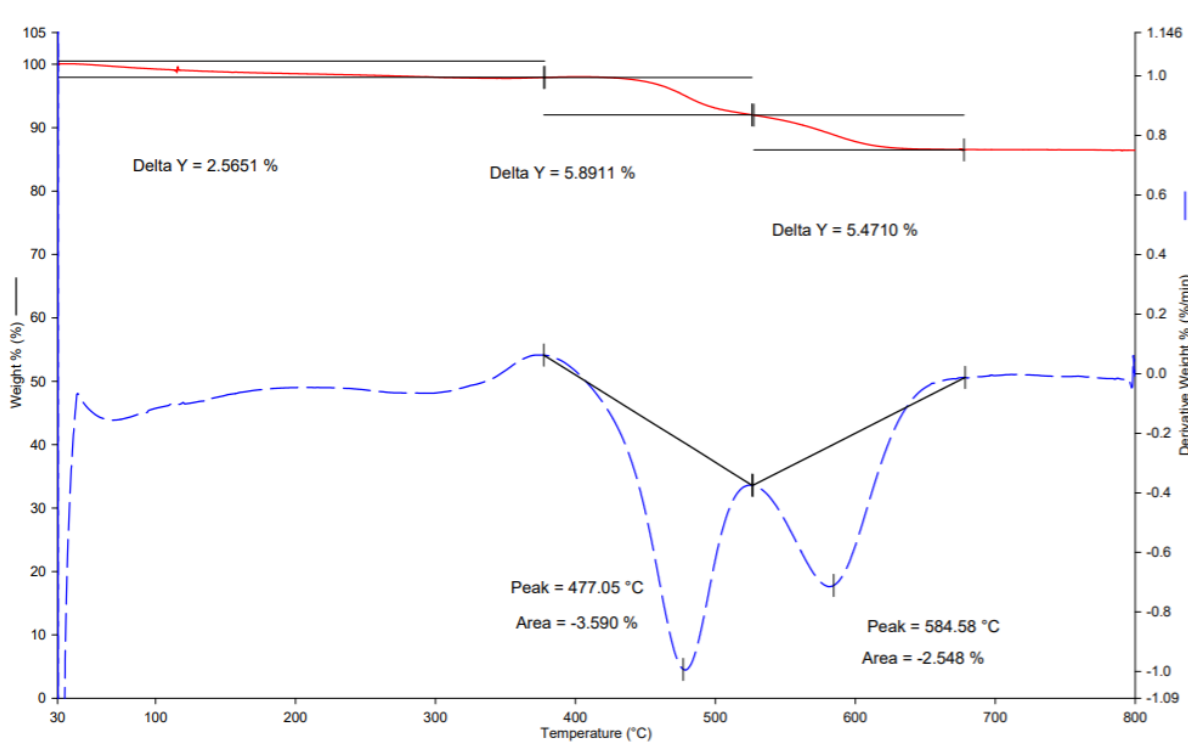


Figure 37: TGA Analysis of spent 6wt% Mo/HZSM-5

The above **Figure 37** shows the results of TGA analysis on a spent 6wt% Mo/HZSM-5 catalyst used in the MDA reaction for two reaction cycles under 95%CH₄ flow for 3h each and 1h of regeneration using pure H₂ between the two cycles. The conditions of this reaction were as

mentioned previously in **Table 6**. According to the literature, these conditions are sufficient to indicate the total amount of coke formed during the MDA reaction. From the thermogram in **Figure 37**, an initial mass loss of about 2.5 wt% is observed in the temperature range of 30 – 300°C, attributed to the oxidation of the active metal sites Mo_2C . The second mass loss of 5.8 wt% was observed with a maximum rate at $\sim 477^\circ\text{C}$, representing the amount of soft coke formed during the reaction. The final mass loss of 5.5 wt.% is observed with a maximum loss rate at 585°C , representing the amount of hard coke that requires a higher temperature to remove. The same analysis was applied to all the spent samples from the experiments on the reaction conditions at different reaction temperatures and space velocities.

Error! Not a valid bookmark self-reference. shows a summary of the TGA results for the experiments mentioned in the previous section. Experiments 1 through 3 were performed under the same reaction and regeneration temperature at 700°C and different space velocities 1875, 3750, and $7500 \text{ ml/g}_{\text{cat}}/\text{h}$. Although the difference is not very noticeable, it can be seen that the higher the space velocity, the smaller the percentage of soft coke and the higher the percentage of hard coke. For the lowest space velocity, the amount of soft coke was higher than that at all the higher space velocities with 6.5wt%. While the amount of hard coke was lower at that space velocity with only 5 wt%.

Table 7: Summary of TGA results for study no. 4

Condition	Reaction/ Regeneration temperature	Space Velocity	Mo ₂ C	Soft Coke	Hard Coke
Experiment No.	°C	ml/g _{cat} /h	wt%	wt%	wt%
1	700	1875	2.9	6.5	5.0
2	700	3750	2.6	5.9	5.5
3	700	7500	2.0	5.8	5.8
4	650	3750	3.3	3.3	2.3
5	750	3750	1.8	9.7	6.6

As mentioned previously in section 2.5, studies claim that soft coke is more accessible to remove during the regeneration phase than hard coke. Therefore, it is more desirable to operate at lower space velocities in this situation to minimize the formation of hard coke. Experiments 2, 4, and 5 were performed under the same space velocity of 3750 ml/g_{cat}/h and different reaction and regeneration temperatures (650, 700, and 750°C). As expected, the lower amount of coke was obtained at the lowest temperature at 650°C with only 3.3wt% soft coke and 2.3wt% hard coke. The amount of both types of coke increases with the increase in temperature, with soft coke being much higher than hard coke. This is due to thermodynamics which results in a higher conversion of methane at higher temperatures. As a result, there is a clear, unavoidable trade-off between the maximum single-pass methane conversion restricted by the reaction temperature and the total amount of coke formed on the catalyst.

6.3.5 Study 5: Periodic Switch Feeding

Periodic Switch Feeding of H₂

Periodic feeding is one of the most promising approaches used in literature to improve the catalyst's performance for the MDA process. The concept behind periodic feeding is to continuously regenerate the catalyst and prevent coke accumulation, potentially killing the catalyst and stopping the process. The benefit of this method is that it allows a semi-continuous process without stopping production for long periods.

In addition, this method, and the pulse feeding method can be used to test the compatibility and identify the maximum and minimum limits of different molecules with the process.

This section includes testing different periodic switch frequencies using H₂. All the experimental conditions applied were as previously mentioned in **Table 6**. The first 30 mins of reaction time were fixed in terms of the feed composition to allow the accumulation of coke. The experiments were performed for 5 hours. A reference experiment was performed with continuous methane feed to observe the change in the performance after applying the periodic switch method.

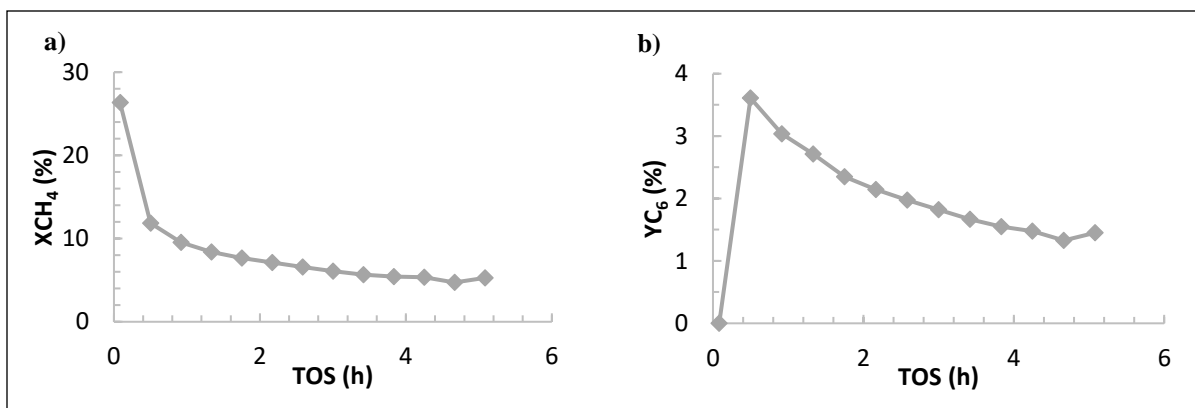


Figure 38: (a) CH₄ conversion (b) and C₆ yield for reference experiment with continuous CH₄ feed

Figure 38 shows the results of the reference experiment where the CH₄ conversion starts very high at around 26% during the induction period, then experiences a sharp decrease to reach 11% after 30 mins of reaction. Then it continues to decrease due to coke formation and accumulation, reaching about 5% by the end of the 5h TOS. While the C₆ yield experiences a maximum after the end of the induction period to reach 3.6%, it then starts to decrease gradually to reach 1.3% by the end of the reaction. This reference experiment has a **D-Slope** of 1.3, which is relatively high compared to the studies in the quantified database. The **Global YC₆** value is 2.5, which falls within the low region, as shown in **Figure 21**, which shows that this factor can be as high as 12 under certain conditions.

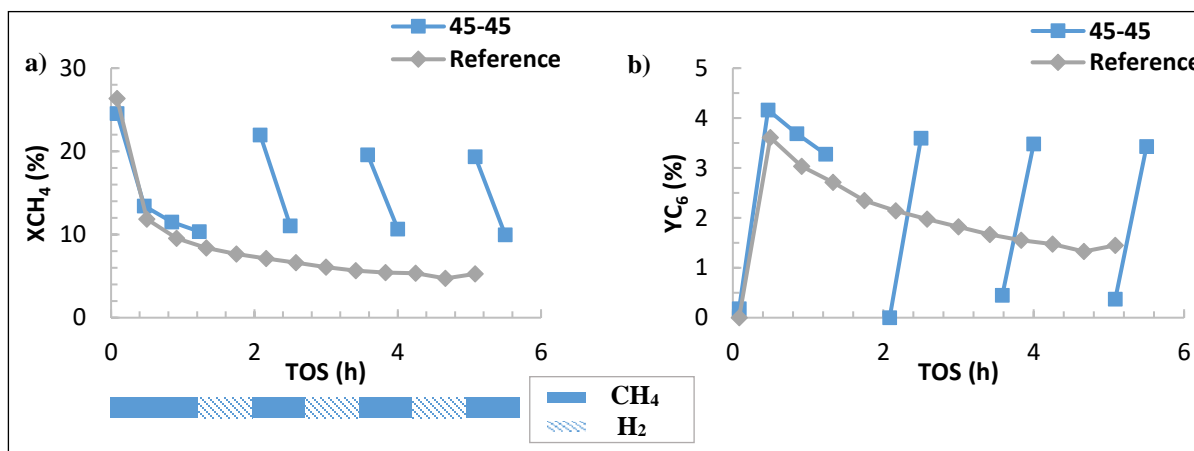


Figure 39: (a) CH₄ conversion (b) and C₆ yield for Reference experiment and 45-45 (min) CH₄-H₂ periodic switch

Figure 39 shows the comparison between the reference case and the periodic switch using H₂ with a switching frequency of 45 mins CH₄ and 45 mins H₂. The line below the conversion plot is to visualize how the feed changed from CH₄ (solid line) to H₂ (striped line) and when the sampling took place throughout the reaction. It can clearly be seen that the use of H₂ results in higher CH₄ conversion throughout the reaction time, although the values highly fluctuated. However, for the C₆ yield, the values fluctuated, with the higher yield corresponding to the lower CH₄ conversion. This means that the high CH₄ conversion indicates the possibility of another induction period following the regeneration step where CH₄ is converted to coke and H₂. These results show that periodic switch using H₂ can be effective. To support that, the **D-Slope** was calculated and found to be 0.7, while the **Global YC₆** is 3.7. Both factors show a significant improvement from the reference experiment and also are closer to the desired goal. However, to understand how much H₂ is required to regenerate the catalyst and how often to introduce it, several other experiments were performed with different frequencies.

Keeping the same reaction time and minimizing the regeneration time to 15 mins only. **Figure 40** shows how the decrease in the regeneration time affects the performance. There is not much difference in the performance between the two experiments. Although the 45-45 (min) CH₄-H₂ switch frequency gives higher performance values, the trend is similar. This indicates that the H₂ exposure time in the 45-15 (min) CH₄-H₂ experiment was almost as efficient as in the 45-45 (min) experiment. This fueled the interest to find the minimum exposure time for H₂ required to maintain the highest performance possible. The **D-Slope** for the 45-15 CH₄-H₂ frequency was found to be 1.2, and the **Global YC₆** is 3.1, which are both lower values than those calculated for the longer regeneration period of 45mins. This is attributed to the long reaction period, which allows the soft coke to take the hard coke form, which is harder to remove. Therefore, to avoid the accumulation of coke, a shorter reaction time of only 15 mins was selected and fixed to test the regeneration ability of H₂.

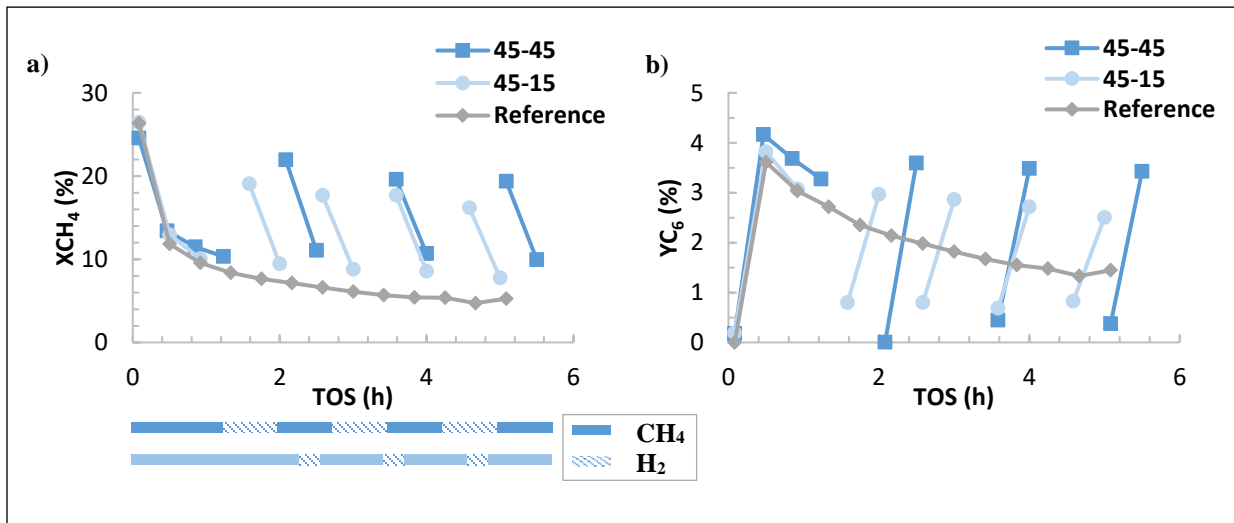


Figure 40: (a) CH₄ conversion (b) and C₆ yield for Reference experiment and 45-45 and 45-15 (min) CH₄-H₂ periodic switch

However, as noticed before, the higher conversion values corresponded to lower yield, tied to the sampling time. The sample that was analyzed at an earlier time of the reaction cycle (after 5 mins) result in higher conversion and lower yield. In contrast, the sample analyzed at the end of the reaction cycle resulted in lower conversion (still within an acceptable range) and higher yield. The low benzene yield does not necessarily indicate bad performance, and it can just mean that the MDA reaction has not started taking place yet. The sampling time is a challenge for shorter reaction cycles as the sampling time for the analysis tool used (GC) is 20.5mins which does not allow multiple injections within the same reaction cycle. Therefore, some work was done to investigate this effect. **Figure 41** explains how where the different data points were sampled. The first sampling time (ST1) was the beginning of the reaction cycle, while the second sampling time (ST2) was at the end of each of the reaction cycles.

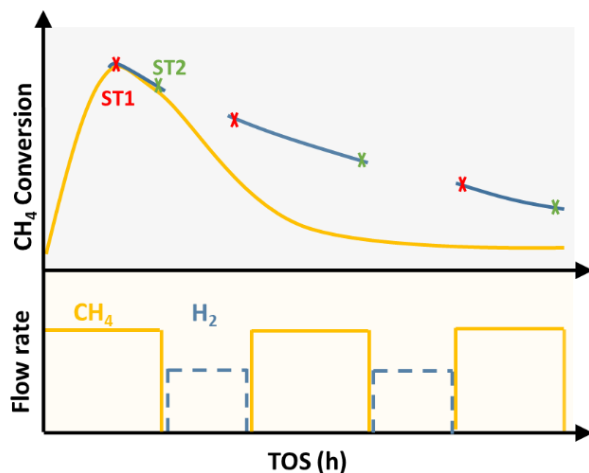


Figure 41: Illustration of the different sampling time (ST1 and ST2) during periodic switch

Two experiments were performed with a periodic switch frequency of 15-5 (min) CH₄-H₂. For the first experiment, the data points were collected at (ST1), while for the second, the data was collected at (ST2).

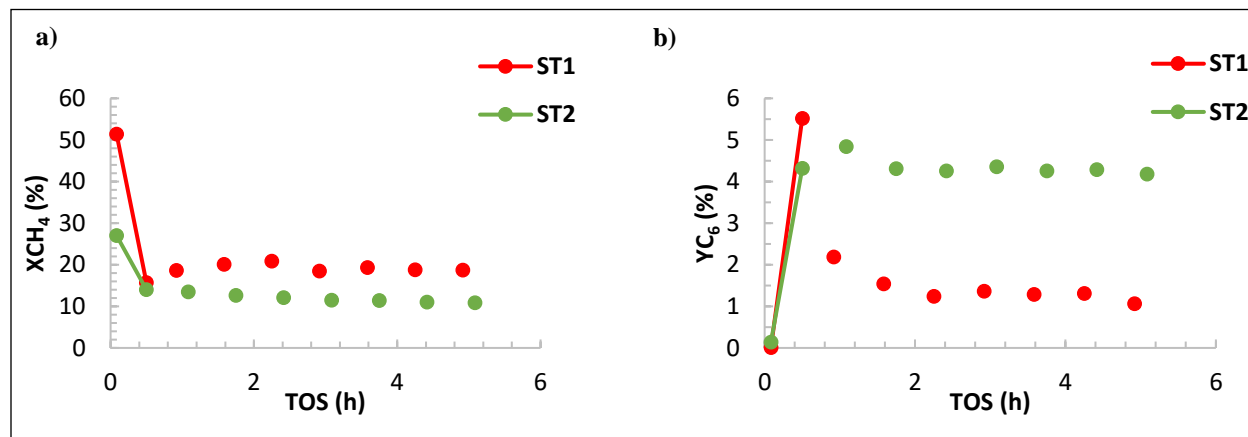


Figure 42: (a) CH₄ conversion (b) and C₆ yield for different sampling times

Figure 42 shows the results of these two experiments. For the results of ST1, the sample was injected into the GC after 5 mins of reaction for a reaction cycle of 15 mins. For the results with the green line, the sample was injected into the GC at the end of the reaction cycle of 15 mins. It can be understood that injecting the sample earlier on during the reaction cycle gives an inaccurate representation of the performance as the conversion is very high while the yield is very low. However, when the sample is injected at the end of the reaction cycle as in ST2, the conversion drops slightly while the yield is much higher. The general conclusion is that for a short reaction cycle, it is better to inject the sample at the end of the reaction cycle so that the comparison between those experiments and an experiment with a longer reaction time where we can inject more than one sample during the reaction, is a fair comparison.

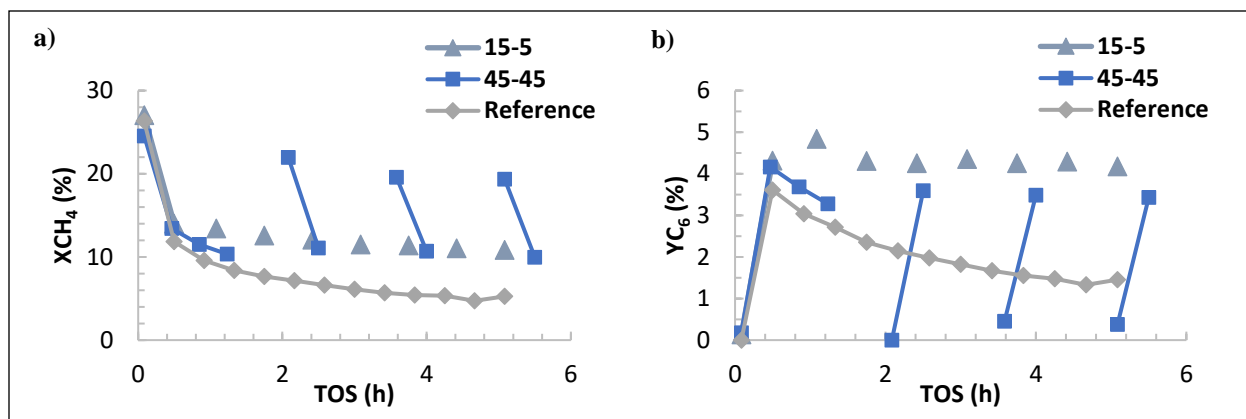


Figure 43: (a) CH₄ conversion (b) and C₆ yield for Reference experiment and 45-45 and 15-5 (min) CH₄-H₂ periodic switch

What can be seen from the above **Figure 43** is that the performance of the shorter reaction time is, in fact, better in terms of maintaining a stable conversion and a higher benzene yield. In both cases, the results show an improvement from the reference experiment with only CH₄ in the feed. The **D-Slope** for the 15-5 CH₄-H₂ frequency is 0.7, which is the same as for the 45-45 CH₄-H₂ experiment and the **Global YC₆** 4.3, which is much higher than the 3.7 for the previous experiment.

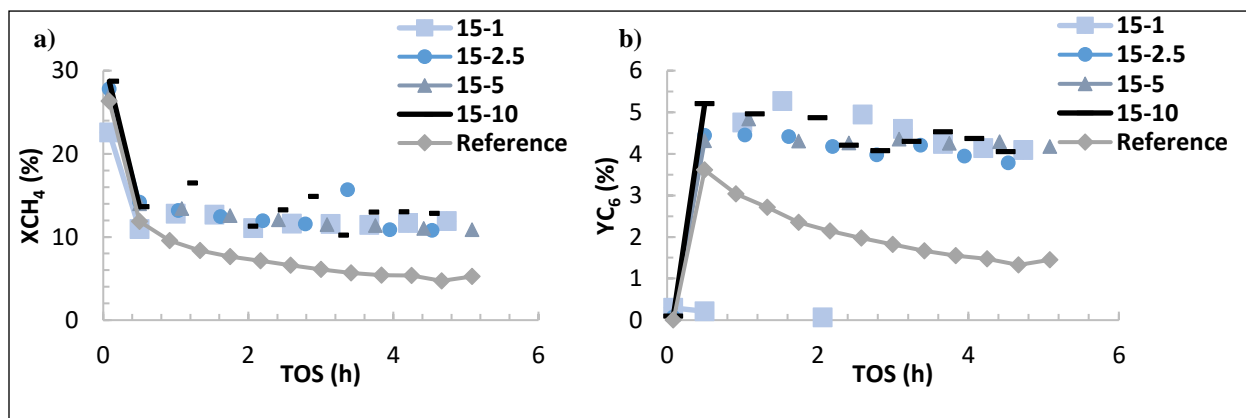


Figure 44: (a) CH₄ conversion (b) and C₆ yield for Reference experiment and 15-1, 15-2.5, 15-5, 15-10 (min) CH₄-H₂ periodic switch

Figure 44 shows the performance of a continuous methane feed compared with a periodic feed of H₂ with CH₄-H₂ 15-5 min. As can be seen, the conversion and yield for the reference experiment continue decreasing over the 5h of reaction. While the periodic feed of H₂ provides a stable performance. Above are the studies done on H₂ periodic feeding to minimize the regeneration time. It can be seen that for a reaction time of 15 min, a range of regeneration time between 10-1 min all perform relatively similarly. Thus, it can be concluded that a periodic feed of CH₄-H₂ with 15-1 min is sufficient for a stable performance. This might indicate that pulsing H₂ can also be efficiently regenerate the coke continuously and provide a stable process. To support that, the results of the **Global YC₆** for each of the experiments are 4.8, 4.2, 4.3, and 4.5, respectively. This shows that 15-1 CH₄-H₂ results in the best average yield while minimizing the regeneration period.

Periodic Switch Feeding of CO₂

To investigate the possibility of achieving oxidative regeneration at the reaction conditions, CO₂ was used as an oxidative molecule in periodic switch mode. Few literature studies showed that introducing CO₂ as a co-fed molecule in minor amounts (2% of the feed) slightly improves the catalyst's performance. This study aims to test the catalyst's ability to withstand pure CO₂ at reaction conditions.

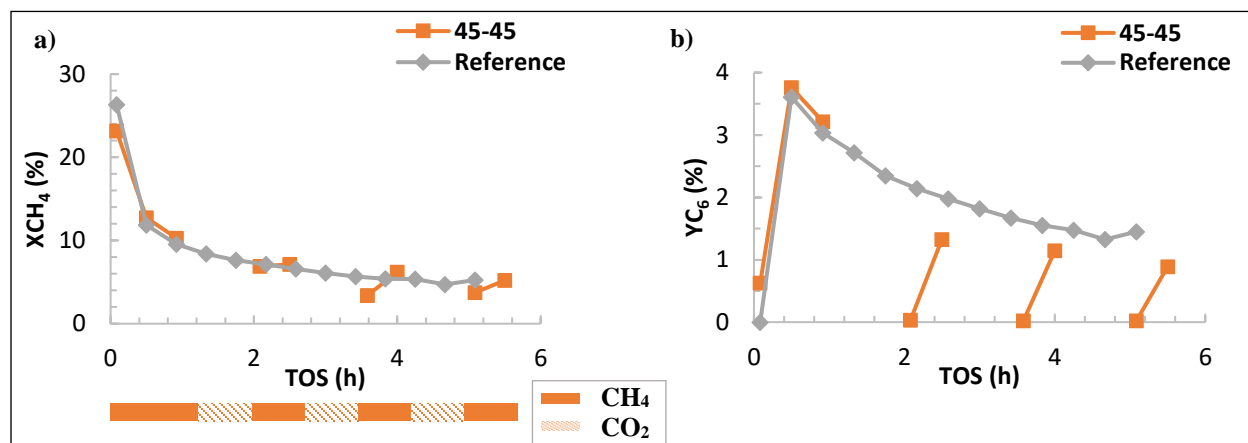


Figure 45: (a) CH₄ conversion (b) and C₆ yield for Reference experiment and 45-45 (min) CH₄-CO₂ periodic switch

Figure 45 shows the effect of the CH₄-CO₂ periodic switch with the frequency of 45-45 (min) while maintaining the same conditions for the temperature and space velocity for both the reaction and the regeneration periods. The results of the periodic switch CH₄-CO₂ are plotted in comparison to the reference experiment. The results show a negative effect of CO₂ on the catalyst performance. Not only did CO₂ not succeed in regenerating the catalyst, but it decreased the selectivity towards aromatics products. This can be seen from the **D-Slope** of 1.5, higher than that of the reference experiment. Moreover, the **Global YC₆** of 1.8 is much lower than the reference.

This can result from CO₂ oxidizing the active metal sites, which requires an additional induction period following each regeneration cycle. Additionally, there is a chance that feeding CO₂ at that high temperature can lead to irreversible deactivation of the active acid-sites, which perform the function of converting the intermediate product to aromatic products. This effect was reported in the literature by Han et al. (2019) when using O₂ as a regenerating molecule at high temperatures. The reaction assumed to occur during the regeneration with CO₂ is the Boudouard reaction, where CO₂ reacts with the coke and forms CO. However, it appears that the reaction of CO₂ with Mo₂C to form MoO_x is dominating. As previously mentioned, the use of CO₂ as the co-fed molecule is very limited, and only minor amounts can be used to avoid irreversibly deactivating the catalyst. It seemed that periodically introducing CO₂ also has the same limitation; therefore, shorter regeneration periods were tested.

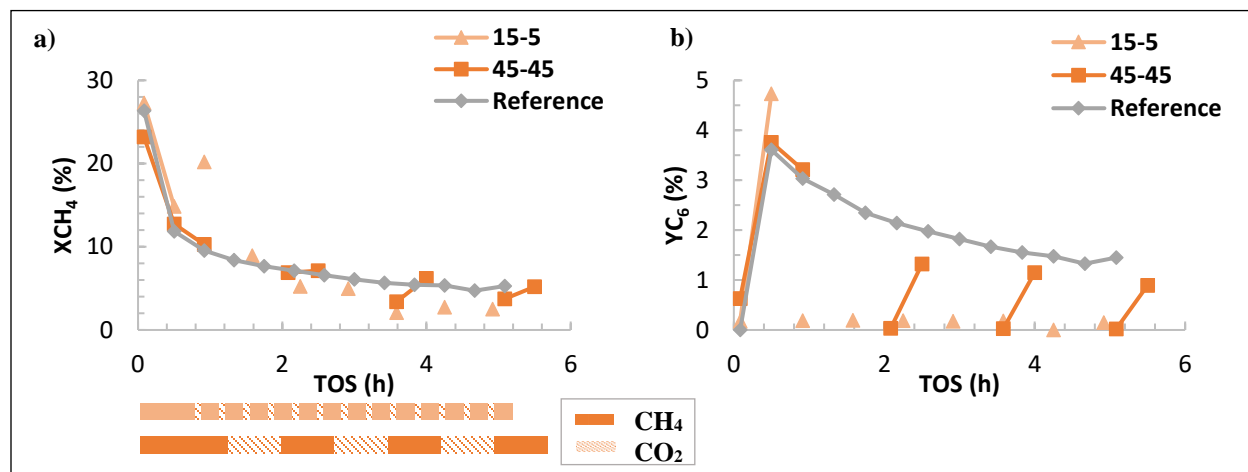


Figure 46: (a) CH₄ conversion (b) and C₆ yield for Reference experiment and 45-45, 15-45, and 15-5 (min) CH₄-CO₂ periodic switch

Figure 46 shows the effect of periodic switch $\text{CH}_4\text{-CO}_2$ at different frequencies in comparison to the reference experiment. Decreasing the reaction time from 45 to 15 mins and the regeneration periods from 45 to 5 mins revealed that CO_2 completely stops the reaction. This shows that the shorter periodic switch frequency resulted in almost the same performance, considering the sampling time. However, the **D-Slope** of 2.8 and the **Global Y_{C_6}** of 1.3 suggest the performance was even worse with a shorter regeneration period. Therefore, we concluded that introducing CO_2 to the MDA process in periodic switch mode has a negative effect on the catalyst performance and was not able to regenerate the coke formed but probably enhanced its formation and re-oxidized the active Mo-carbide sites, which led to a decrease in the methane conversion.

Periodic Switch Feeding of H_2+CO_2

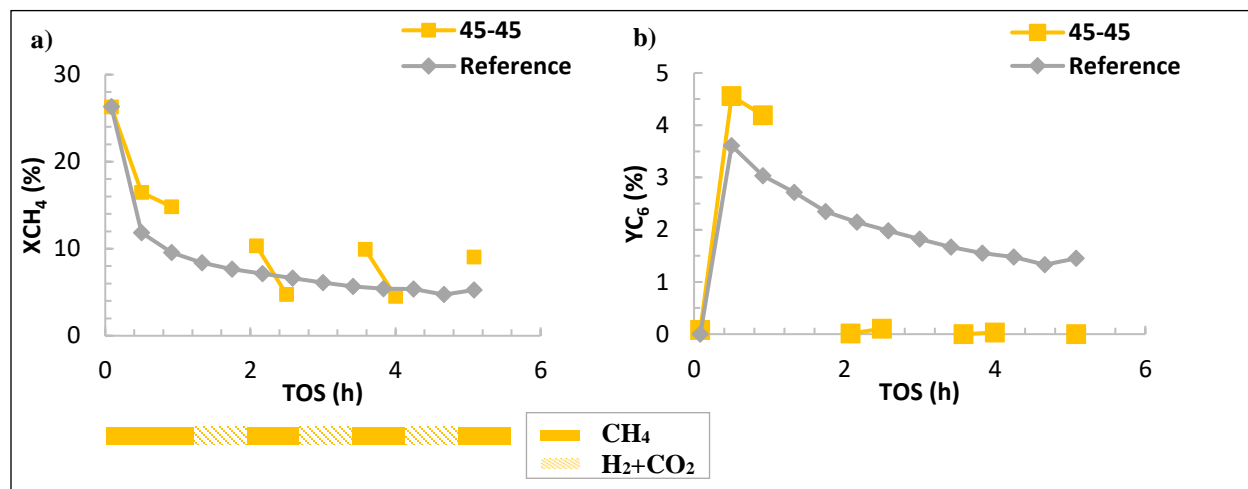


Figure 47: (a) CH_4 conversion (b) and C_6 yield for Reference experiment and 45-45 (min) $\text{CH}_4\text{-H}_2+\text{CO}_2$ periodic switch

Another goal of this work was to combine both reductive and oxidative catalyst regeneration. Therefore, CO_2 and H_2 were combined with a 1:1 ratio to explore this possibility.

Figure 47 shows the effect of the periodic switch of CH_4 - H_2 + CO_2 with a frequency of 45-45 (min) in comparison to the reference experiment. As can be seen, the combination of CO_2 and H_2 during regeneration leads to a significant decrease in the performance, leading to almost no aromatics formation. Instead of regenerating the catalyst, the molecules reacted and formed water molecules during the regeneration period, which was observed as droplets at the bottom end of the reactor, which is exposed to room temperature. The **D-Slope** was 1.6, while the **Global Y_{C_6}** was the lowest reported value of 1.1. A reverse water-gas-shift reaction is assumed to have taken place, The produced water can be one of the reasons for the suppression of aromatics formation. It was observed in the literature that water negatively impacts the MDA reaction. Other frequencies were tested, and the same results were obtained. It can be concluded that combining CO_2 and H_2 with a 1:1 ratio was insufficient to regenerate the catalyst.

6.3.6 Study 6: Pulse Feeding with H_2 and CO_2

An alternative method to test the compatibility of certain gases with the MDA process is pulse feeding. This method is very useful, especially if these gases are not favorable and have limited use. In addition, this method can allow the rate of regeneration to be similar to the rate of deactivation, which is critical due to the assumption that coke is easier to remove when it is in the soft-coke form, which can then turn into hard-coke form if not removed fast enough.

This method was applied in a study done by Kosinov et al. (2016) using pure O_2 , and led to an improvement in the total benzene yield compared to the pure methane feed as it allowed the reaction to go for 16h until in comparison to 8h only for the pure methane feed.

Pulse Feeding of H₂

The reason behind using H₂ in pulses instead of co-feeding is that H₂ is one of the products of the MDA reaction, which makes it thermodynamically unfavorable. However, its ability to remove coke and maintain a stable process has been proven from the periodic switch mode, which makes pulsing H₂ the middle point that allows using H₂ without the need to stop the reaction for a separate regeneration step.

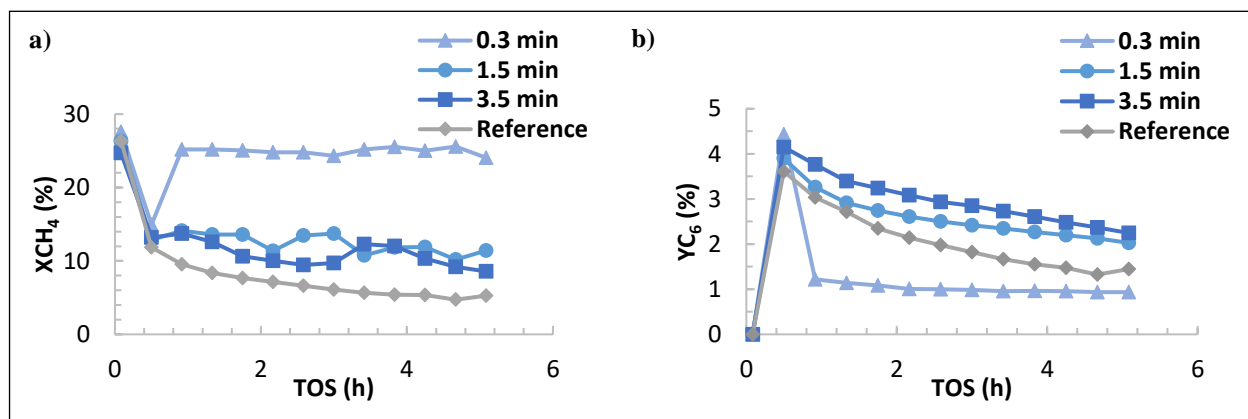


Figure 48: (a) CH₄ conversion (b) and C₆ yield for Reference experiment and H₂ pulsing with 0.3, 1.5, and 3.5 min frequencies

The results shown in **Figure 48** are for the MDA reaction with H₂ pulsing every 0.3, 1.5, and 3.5 mins. The experiment with H₂ pulsing every 0.3min gives a very high methane conversion but much lower benzene yield than the reference experiment. This means that H₂ is most likely reacting with the methane with this frequency before it reaches the active sites, not allowing the MDA process to occur. However, it is important to note that the results are very stable for the 5h reaction period, which could mean that the very frequent pulsing suppressed coke formation.

As a result, the frequency was changed to pulsing every 1.5min, which resulted in lower methane conversion; however, still higher than the reference point. While the benzene yield was

higher and more stable than the reference experiment. Then, the frequency was reduced to 3.5min, and the results showed a methane conversion very similar to the previous experiment and a slightly higher benzene yield. These results indicate that H₂ pulsing could be a very promising approach to maintain a stable process. However, when compared to the CH₄-H₂ periodic switch shown in **Figure 49**, it can be seen that the performance is much more stable, and the benzene yield is significantly higher for the periodic switch.

To further support these results, the **D-Slope** was 0.2, 0.3, and 1, respectively. However, the **Global YC₆** values are 1.9, 2.8, and 3, for pulsing frequency of 0.3, 1.5, and 3.5 mins, respectively. Although the **D-Slope** results indicated the lowest frequency provides the most stable performance, the **Global YC₆** reveals that this condition does not result in a sufficient production of benzene. However, compared to the results of the periodic switch method, it is clear that the H₂ pulsing method is less efficient.

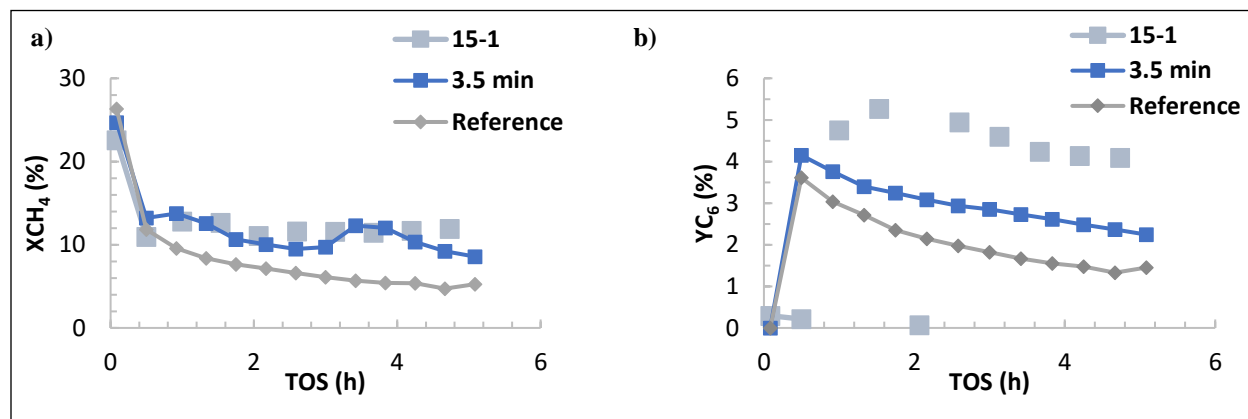


Figure 49: (a) CH₄ conversion (b) and C₆ yield for Reference experiment and 15-1 (min) CH₄-H₂ periodic switch and H₂ pulsing with frequency of 3.5 min

Pulse Feeding of CO₂

The results of the periodic feeding of CO₂ showed that it is not compatible with the MDA process; however, natural gas, which is the main feed for the MDA process, is in reality always accompanied by CO₂. Therefore, it is essential to find the maximum limit of CO₂ that the process can withstand under the reaction conditions and the catalyst used in this study. Investigating the CO₂ pulsing technique is one way to identify this limit.

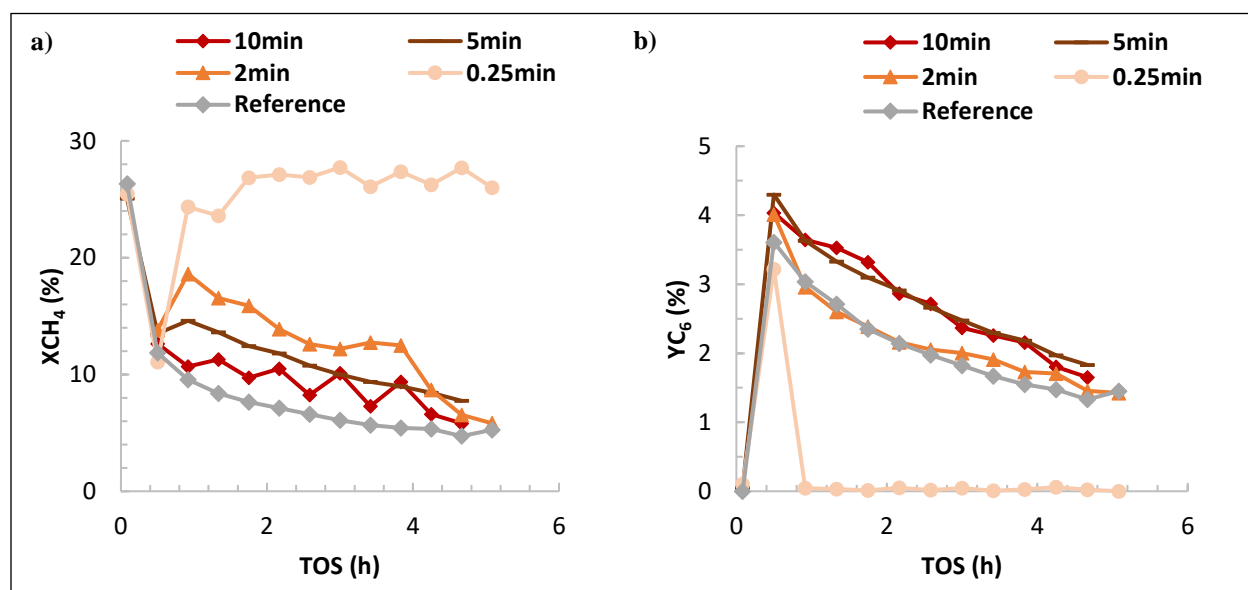


Figure 50: (a) CH₄ conversion (b) and C₆ yield for Reference experiment and CO₂ pulsing with 0.25, 2, 3.5, 5, and 10 mins frequencies

Figure 50 shows the effect of pulsing CO₂ throughout the MDA process with different frequencies varying from 0.25 to 10 mins. Pulsing CO₂ at the highest frequency of 0.25min resulted in very high CH₄ conversion, which is much higher than the thermodynamic limitations for the MDA reaction, which means that it is highly likely that the MDA reaction did not occur. This was very clear from the results of the benzene yield, which shows that no benzene was formed

throughout the entire time on stream. Then the pulsing frequency was decreased to 2mins, which showed a decrease in the methane conversion from the previous experiment while the benzene yield almost matched the reference point. This shows that pulsing CO₂ every 2 mins did not regenerate the catalyst at all. Instead, the CO₂ reacted with the main methane feed. The frequency was decreased even further to pulsing every 5mins. This showed a lower methane conversion than previous trials but a higher benzene yield. Reducing the pulsing frequency to 10 mins resulted in very similar results. However, the stability of the process, as implied by the rate of decrease in the methane conversion or benzene yield, was not improved in any of the experiments. To support that are the results of the **D-Slope** for the pulsing frequencies 10, 5, and 2 mins, which are 1.6, 1.5, and 1.7, respectively. The **D-Slope** values are all higher than the reference experiment indicating that the use of any amount of CO₂ will definitely have a negative effect on the stability of the catalyst. As for the **Global YC₆**, the results are very similar, ranging between 2.4 and 2.7, which is similar to the reference experiment. This indicates that the Mo/HZSM-5 catalyst could not withstand the oxidizing molecule (CO₂) at the reaction conditions, regardless of the feeding technique.

7. CONCLUSION AND FUTURE RECOMMENDATIONS

To conclude, this work focused on the deactivation challenge associated with the Methane Dehydroaromatization process. The work started with an intensive literature review that was then utilized to create a quantified database that included information about the catalyst performance in reactant (CH₄) conversion and product yield and selectivity under different process conditions. These data were used to understand the effect of the different conditions such as Mo content, Si/Al ratio, reaction temperature, and reaction space velocity. The claims in the literature about the impact of each of these factors were addressed and tested.

Two new parameters were generated from the data. These parameters are the **D-Slope** that test the stability of the performance and the **Global YC₆** that compare to total benzene production. These factors were excellent indicators of the catalyst's stability and productivity under the specific reaction conditions. They help judge and compare the performance of any new catalyst to be tested for this process or any new conditions that may be suggested.

Furthermore, unconventional regeneration methods, i.e., periodic switch feeding and pulse feeding, were developed and tested experimentally to examine the compatibility of new gases that can be used to regenerate the MDA catalyst. The gases used in this work are H₂ as a reductive molecule and CO₂ as an oxidative molecule. A reference experiment was performed to monitor the effect of the process conditions. This experiment had a **D-Slope** of 1.3 and a **Global YC₆** of 2.5.

The periodic switch feeding results using CH₄-H₂ showed the best performance with the highest stability and an average benzene production with a **D-slope** of 0.2 and a **Global YC₆** of 4.8. Using H₂ in pulses positively affected the performance, but with it being thermodynamically

unfavorable, the results were lower than the periodic switch feeding of CH₄-H₂. The catalyst showed almost no activity towards the MDA challenge after introducing CO₂ in a periodic mode at the reaction conditions. However, it provided some regeneration ability when introduced in pulse mode, but it was not significant. The possibility of combining reductive and oxidative regeneration under the same conditions was also tested and resulted in other undesired reactions, such as water-gas-shift reaction producing water, which reportedly has a negative impact on the catalytic activity.

The quantified database created in this work can become a powerful tool to identify the hidden correlations between the different process variables and conditions in the field of MDA reaction. Therefore, it is suggested to use statistical analysis to find these correlations, which cannot be found through the conventional methods given a large number of data points. Furthermore, the results of this work show that Mo/ZSM-5 is incapable of withstanding CO₂, which is an unavoidable composition of natural gas. Therefore, it is recommended for future work in this field to focus on synthesizing a catalyst that can handle CO₂.

It is recommended for future work in this field to synthesize a catalyst that can withstand CO₂ as it is an unavoidable composition of natural gas. In addition, the testing protocols developed in this work using pulse and periodic-switch feeding can be used in the future to study the impact of other molecules on different processes.

8. REFERENCES

- Abedin, M. A., Kanitkar, S., Bhattar, S., & Spivey, J. J. (2020). Sulfated hafnia as a support for Mo oxide: A novel catalyst for methane dehydroaromatization. *Catalysis Today*, 343(February 2019), 8–17. <https://doi.org/10.1016/j.cattod.2019.02.021>
- About-Gheit, A. K., & Awadallah, A. E. (2009). Effect of combining the metals of group VI supported on H-ZSM-5 zeolite as catalysts for non-oxidative conversion of natural gas to petrochemicals. *Journal of Natural Gas Chemistry*, 18(1), 71–77. [https://doi.org/10.1016/S1003-9953\(08\)60080-8](https://doi.org/10.1016/S1003-9953(08)60080-8)
- Blumberg, L. M. (2012). 2.1. introduction. In C. Poole (Ed.), *Gas Chromatography* (p. 20). Retrieved from <https://ebookcentral.proquest.com/lib/tamucs/detail.action?docID=943706>.
- Chen, M., Song, Y., Liu, B., Liu, X., Xu, Y., & Zhang, Z. G. (2020). Experimental investigation of the promotion effect of CO on catalytic behavior of Mo/HZSM-5 catalyst in CH₄ dehydroaromatization at 1073 K. *Fuel*, 262(November 2019), 116674. <https://doi.org/10.1016/j.fuel.2019.116674>
- Dagle, R., Dagle, V., Bearden, M., Holladay, J., Krause, T., & Ahmed, S. (2017). *An Overview of Natural Gas Conversion Technologies for Co-Production of Hydrogen and Value-Added Solid Carbon Products*. Retrieved from <https://www.osti.gov/servlets/purl/1411934>
- Dutta, K., Li, L., Gupta, P., Gutierrez, D. P., & Kopyscinski, J. (2018). Direct non-oxidative methane aromatization over gallium nitride catalyst in a continuous flow reactor. *Catalysis Communications*, 106(December 2017), 16–19. <https://doi.org/10.1016/j.catcom.2017.12.005>

- Fila, V., Bernauer, M., Bernauer, B., & Sobalik, Z. (2015). Effect of addition of a second metal in Mo/ZSM-5 catalyst for methane aromatization reaction under elevated pressures. *Catalysis Today*, 256(P2), 269–275. <https://doi.org/10.1016/j.cattod.2015.02.035>
- Han, S. J., Kim, S. K., Hwang, A., Kim, S., Hong, D. Y., Kwak, G., ... Kim, Y. T. (2019). Non-oxidative dehydroaromatization of methane over Mo/H-ZSM-5 catalysts: A detailed analysis of the reaction-regeneration cycle. *Applied Catalysis B: Environmental*, 241(April 2018), 305–318. <https://doi.org/10.1016/j.apcatb.2018.09.042>
- Honda, K., Yoshida, T., & Zhang, Z. G. (2003). Methane dehydroaromatization over Mo/HZSM-5 in periodic CH₄-H₂ switching operation mode. *Catalysis Communications*, 4(1), 21–26. [https://doi.org/10.1016/S1566-7367\(02\)00242-X](https://doi.org/10.1016/S1566-7367(02)00242-X)
- Ismagilov, Z.R., Tsikoza, L. T., Matus, E. V., Litvak, G. S., Ismagilov, I. Z., & Sukhova, O. B. (2017). Carbonization and Regeneration of Mo/ZSM-5 Catalysts for Methane Dehydroaromatization. *Eurasian Chemico-Technological Journal*, 7(2), 115. <https://doi.org/10.18321/ectj622>
- Ismagilov, Zinifer R., Matus, E. V., & Tsikoza, L. T. (2008). Direct conversion of methane on Mo/ZSM-5 catalysts to produce benzene and hydrogen: Achievements and perspectives. *Energy and Environmental Science*, 1(5), 526–541. <https://doi.org/10.1039/b810981h>
- Jeong, J., Hwang, A., Kim, Y. T., Hong, D. Y., & Park, M. J. (2020). Kinetic modeling of methane dehydroaromatization over a Mo₂C/H-ZSM5 catalyst: Different deactivation behaviors of the Mo₂C and H-ZSM5 sites. *Catalysis Today*, 352(August 2019), 140–147. <https://doi.org/10.1016/j.cattod.2019.09.002>
- Julian, I., Roedern, M. B., Hueso, J. L., Irusta, S., Baden, A. K., Mallada, R., ... Santamaria, J.

- (2020). Supercritical solvothermal synthesis under reducing conditions to increase stability and durability of Mo/ZSM-5 catalysts in methane dehydroaromatization. *Applied Catalysis B: Environmental*, 263(November 2019), 118360. <https://doi.org/10.1016/j.apcatb.2019.118360>
- Karakaya, C., & Kee, R. J. (2016). Progress in the direct catalytic conversion of methane to fuels and chemicals. *Progress in Energy and Combustion Science*, 55, 60–97. <https://doi.org/10.1016/j.pecs.2016.04.003>
- Klee, M. S. (2012). Detectors. In C. Poole (Ed.), *Gas Chromatography* (p. 308). <https://doi.org/10.1016/B978-0-12-385540-4.00012-2>
- Kosinov, N., Coumans, F. J. A. G., Uslamin, E., Kapteijn, F., & Hensen, E. J. M. (2016). Selective Coke Combustion by Oxygen Pulsing During Mo/ZSM-5-Catalyzed Methane Dehydroaromatization. *Angewandte Chemie*, 128(48), 15310–15314. <https://doi.org/10.1002/ange.201609442>
- Kosinov, N., & Hensen, E. J. M. (2020). Reactivity, Selectivity, and Stability of Zeolite-Based Catalysts for Methane Dehydroaromatization. *Advanced Materials*. <https://doi.org/10.1002/adma.202002565>
- Lasobras, J., Soler, J., Herguido, J., Menéndez, M., Jimenez, A., da Silva, M., ... Lázaro, J. (2019). Methane aromatization in a fluidized bed reactor: Parametric study. *Frontiers in Energy Research*, 7(FEB). <https://doi.org/10.3389/fenrg.2019.00008>
- Li, Y., Su, L., Wang, H., Liu, H., Shen, W., Bao, X., & Xu, Y. (2003). Combined single-pass conversion of methane via oxidative coupling and dehydroaromatization. *Catalysis Letters*, 89(3–4), 275–279. <https://doi.org/10.1023/A:1025723000836>

- Liu, Y., Kooli, F., & Borgna, A. (2019). Tandem dual bed Mo/HZSM-5 and Mo/HMCM-22 catalysts with enhanced catalytic performance for natural gas conversion to aromatics. *Catalysis Today*, (December 2018), 0–1. <https://doi.org/10.1016/j.cattod.2019.09.026>
- Ma, S., Guo, X., Zhao, L., & Scott, S. (2013). Recent progress in methane dehydroaromatization : From laboratory curiosities to promising technology. *Journal of Energy Chemistry*, 22(1), 1–20. [https://doi.org/10.1016/S2095-4956\(13\)60001-7](https://doi.org/10.1016/S2095-4956(13)60001-7)
- Majhi, S., & Mohanty, P. (2013). Direct conversion of natural gas to higher hydrocarbons : A review. *Journal of Energy Chemistry*, 22(4), 543–554. [https://doi.org/10.1016/S2095-4956\(13\)60071-6](https://doi.org/10.1016/S2095-4956(13)60071-6)
- Portilla, M. T., Llopis, F. J., & Martínez, C. (2015). Non-oxidative dehydroaromatization of methane: An effective reaction-regeneration cyclic operation for catalyst life extension. *Catalysis Science and Technology*, 5(7), 3806–3821. <https://doi.org/10.1039/c5cy00356c>
- Qi, S., & Yang, B. (2004). *Methane aromatization using Mo-based catalysts prepared by microwave heating*. 98, 639–645. <https://doi.org/10.1016/j.cattod.2004.09.049>
- Ravi, M., Ranocchiari, M., & van Bokhoven, J. A. (2017). The Direct Catalytic Oxidation of Methane to Methanol—A Critical Assessment. *Angewandte Chemie - International Edition*, 56(52), 16464–16483. <https://doi.org/10.1002/anie.201702550>
- Schwach, P., Pan, X., & Bao, X. (2017). Direct Conversion of Methane to Value-Added Chemicals over Heterogeneous Catalysts: Challenges and Prospects. *Chemical Reviews*, 117(13), 8497–8520. <https://doi.org/10.1021/acs.chemrev.6b00715>
- Skutil, K., & Taniewski, M. (2006). Some technological aspects of methane aromatization (direct and via oxidative coupling). *Fuel Processing Technology*, 87(6), 511–521.

<https://doi.org/10.1016/j.fuproc.2005.12.001>

- Sridhar, A., Rahman, M., Infantes-Molina, A., Wylie, B. J., Borcik, C. G., & Khatib, S. J. (2020). Bimetallic Mo-Co/ZSM-5 and Mo-Ni/ZSM-5 catalysts for methane dehydroaromatization: A study of the effect of pretreatment and metal loadings on the catalytic behavior. *Applied Catalysis A: General*, 589(June 2019), 117247. <https://doi.org/10.1016/j.apcata.2019.117247>
- Sun, C., Fang, G., Guo, X., Hu, Y., Ma, S., Yang, T., ... Bao, X. (2015). Methane dehydroaromatization with periodic CH₄-H₂ switch: A promising process for aromatics and hydrogen. *Journal of Energy Chemistry*, 24(3), 257–263. [https://doi.org/10.1016/S2095-4956\(15\)60309-6](https://doi.org/10.1016/S2095-4956(15)60309-6)
- Sun, L., Wang, Y., Guan, N., & Li, L. (2019). *Methane Activation and Utilization : Current Status and Future Challenges*. 1(1), 1–13. <https://doi.org/10.1002/ente.201900826>
- Taifan, W., & Baltrusaitis, J. (2016). CH₄ conversion to value added products: Potential, limitations and extensions of a single step heterogeneous catalysis. *Applied Catalysis B: Environmental*, 198, 525–547. <https://doi.org/10.1016/j.apcatb.2016.05.081>
- Tessonnier, J. P., Louis, B., Rigolet, S., Ledoux, M. J., & Pham-Huu, C. (2008). Methane dehydroaromatization on Mo/ZSM-5: About the hidden role of Brønsted acid sites. *Applied Catalysis A: General*, 336(1–2), 79–88. <https://doi.org/10.1016/j.apcata.2007.08.026>
- Uslamin, E. A., Saito, H., Sekine, Y., Hensen, E. J. M., & Kosinov, N. (2020). Different mechanisms of ethane aromatization over Mo/ZSM-5 and Ga/ZSM-5 catalysts. *Catalysis Today*, (March), 1–9. <https://doi.org/10.1016/j.cattod.2020.04.021>
- Vollmer, I., Yarulina, I., Kapteijn, F., & Gascon, J. (2019a). *Progress in Developing a Structure-Activity Relationship for the Direct Aromatization of Methane*. 39–52.

<https://doi.org/10.1002/cctc.201800880>

Vollmer, I., Yarulina, I., Kapteijn, F., & Gascon, J. (2019b). Progress in Developing a Structure-Activity Relationship for the Direct Aromatization of Methane. *ChemCatChem*, *11*(1), 39–52. <https://doi.org/10.1002/cctc.201800880>

Xu, Yide, Bao, X., & Lin, L. (2003). Direct conversion of methane under nonoxidative conditions. *Journal of Catalysis*, *216*(1–2), 386–395. [https://doi.org/10.1016/S0021-9517\(02\)00124-0](https://doi.org/10.1016/S0021-9517(02)00124-0)

Xu, Yide, & Lin, L. (1999). *Recent advances in methane dehydro-aromatization over transition metal ion-modified zeolite catalysts under non-oxidative conditions*. *188*, 53–67.

Xu, Yuebing, Chen, M., Liu, B., Jiang, F., & Liu, X. (2020). CH₄ conversion over Ni/HZSM-5 catalyst in the absence of oxygen: Decomposition or dehydroaromatization? *Chemical Communications*, *56*(32), 4396–4399. <https://doi.org/10.1039/d0cc01345e>

Xu, Yuebing, Lu, J., Suzuki, Y., Zhang, Z., & Ma, H. (2013). Chemical Engineering and Processing: Process Intensification Performance of a binder-free, spherical-shaped Mo / HZSM-5 catalyst in the non-oxidative CH₄ dehydroaromatization in fixed- and fluidized-bed reactors under periodic CH₄ – H₂ switch operati. *Chemical Engineering & Processing: Process Intensification*, *72*, 90–102. <https://doi.org/10.1016/j.cep.2013.05.016>

Xu, Yuebing, Lu, J., Wang, J., Suzuki, Y., & Zhang, Z. G. (2011). The catalytic stability of Mo/HZSM-5 in methane dehydroaromatization at severe and periodic CH₄-H₂ switch operating conditions. *Chemical Engineering Journal*, *168*(1), 390–402. <https://doi.org/10.1016/j.cej.2011.01.047>

Xu, Yuebing, Song, Y., & Zhang, Z. (2016). A binder-free fluidizable Mo/HZSM-5 catalyst for non-oxidative methane dehydroaromatization in a dual circulating fluidized bed reactor

- system. *Catalysis Today*. <https://doi.org/10.1016/j.cattod.2016.03.037>
- Xu, Yuebing, Wang, J., Suzuki, Y., & Zhang, Z. G. (2012). Improving effect of Fe additive on the catalytic stability of Mo/HZSM-5 in the methane dehydroaromatization. *Catalysis Today*, *185*(1), 41–46. <https://doi.org/10.1016/j.cattod.2011.09.026>
- Xue, J., Chen, Y., Wei, Y., Wang, H., & Caro, J. (2016). *Gas to Liquids: Natural Gas Conversion to Aromatic Fuels and Chemicals in a Hydrogen-Permeable Ceramic Hollow Fiber Membrane Reactor*. *2451*(1), 2448–2451. <https://doi.org/10.1021/acscatal.6b00004>
- Zhang, Z.-G. (2019). Process, reactor and catalyst design: Towards application of direct conversion of methane to aromatics under nonoxidative conditions. *Carbon Resources Conversion*, *2*(3), 157–174. <https://doi.org/10.1016/j.crcon.2019.07.001>
- ZSM-5 | Zeolyst International Zeolyst International. (n.d.). Retrieved April 20, 2021, from <https://www.zeolyst.com/our-products/standard-zeolite-powders/zsm-5.html>